A WIDE-AREA CONTROL FOR MITIGATING ANGLE INSTABILITY IN ELECTRIC POWER SYSTEMS

By

DONGCHEN HU

A thesis submitted in partial fulfillment of

the requirements for the degree of

MASTER OF SCIENCE IN ELECTRICAL ENGINEERING

WASHINGTON STATE UNIVERSITY

School of Elecrtical Engineering and Computer Science

DECEMBER 2006

To the Faculty of Washington State University:

The members of the Committee appointed to examine the thesis of DONGCHEN HU find it satisfactory and recommend that it be accepted.

_____
Chair

_____

_____

_____

ACKNOWLEDGMENT

I would like to express my sincere gratitude to my advisor Professor Vaithianathan Venkatasubramanian for his guidance, enlightening instruction and support throughout my study at Washington State University.

I wish to thank Professor Anjan Bose and Professor Kevin Tomsovic for their instruction and valuable discussions on this work, and Professor Carl Hauser for his constructive and valuable interest. I also want to say thanks to all the other professors who have helped me during my studies here.

Support from Power Systems Engineering Research Center (PSERC), Consortium for Electric Reliability Technology Solutions (CERTS), and Bonneville Power Administration (BPA) is gratefully acknowledged.

A WIDE-AREA CONTROL FOR MITIGATING ANGLE INSTABILITY IN ELECTRIC POWER SYSTEMS

ABSTRACT

by Dongchen Hu, M.S.
Washington State University
December 2006

Chair: Vaithianathan Venkatasubramanian

Power system operation is undergoing major technological advances with many new installations of synchrophasors all across the North American grid as well in power systems all over the world. Wide-area monitoring system (WAMS) in the Pacific Northwest and Eastern Interconnection Phasor Project (EIPP) are examples of such installations. Synchrophasors together with modern communication technology facilitate the monitoring of the current state of the power system including the phase angles of bus voltage at critical buses in a coordinated fashion.

Power system operation is constantly facing contingencies such as from line faults and generator outages. For operational reliability, the system must be able to withstand the contingencies, either by itself (for N-1 contingency) or with the help of Special Protection Schemes (SPS) or Remedial Action Schemes (for N-2 or worse contingencies). However, when the system is operating under unforeseen conditions or under unusually high stress, the system can undergo angle instability. In that case, the system breaks up into many islands resulting in large loss of loads and generations and a potential black-out scenario. In this thesis, new algorithms are proposed for detecting the emergence of

angle instability phenomena while it is still emerging so that suitable countermeasures can be initiated to prevent the islanding.

The proposed algorithms and the controller detect the fast separation of phase angles among the critical areas automatically using the synchrophasors and proceed to mitigate the instability by suitable switching action. The transient energy method is also used to solve the problem in this thesis. The thesis will discuss the new algorithms along with illustrative examples on standard IEEE test systems.

TABLE OF CONTENTS

LIST OF TABLES

LIST OF FIGURES

CHAPTER 1 INTRODUCTION

The dynamic responses of power systems can vary over vastly different timescales, ranging from milliseconds to minutes and even hours. For each type of these dynamic phenomena, separate controllers have been designed to ensure uninterrupted reliable operation of the electric power grid that consists of transmission lines, synchronous machines and consumer loads. The basic control actions, such as the ultra fast power system protection as well as the slower excitation and governor controls, have been well developed over the previous decades [5][6]. In the past, the power systems were designed so that most of the controls were based on local measurements. But on the other hand, during severely stressed cases, the local control schemes can potentially work against each other, gradually pushing the system towards cascading outages. Under such severe and unusual opening conditions, local controls alone can not solve the system security problems. There have been many recent instances of large-scale blackouts all over the world [1-4]. These blackouts point to the need for wide-area controls since the blackouts have highlighted the limitations of the local-based actions.

Power systems are large interconnected nonlinear systems where system wide instabilities or collapses do occur over time. Accordingly, operator actions together with automatic control actions are designed to prevent or minimize the damage caused by such outages. The power-flows across distant parts of the system have been growing steadily to meet the ever increasing consumer demands. But, the investment into new transmission lines has been limited due to economic as well as environmental concerns. Therefore, the steady growth of consumer demands is gradually stressing the electric

power system more and more. As a result, the system operation can find itself close to or outside the secure operating limits under severe contingencies.

From the technology perspective, there has been spectacular growth in the past twenty years from advances in computer and communication sciences. These advances provide the opportunity for feasible and economical implementation of wide-area controls in the electric power system.

Wide-area measurement and control systems present a new solution which can be integrated easily and cost effectively into the power grid. A wide-area control system can provide the ability to increase the power transmission capability and also improve the system reliability. Many recent publications have analyzed the requirements and designs of wide-area controls. The setup and applications of comprehensive wide-area systems are introduced in [7-9]. The whole new control system can identify critical situations and determine appropriate remedial actions. The identification together with the actions can be notified to the operator, and closed loop fast control actions can also be taken automatically depending on the time frame of the event.

One of the earliest applications of wide-area feedback control in the power system is the load frequency control [10-12] that was developed in the 1970's. Any imbalance between generation and load will cause the deviation of the system frequency away from the nominal 60 Hz. A secondary control loop, called the Automatic Generation Control, (AGC), coordinates the individual governor responses of the generators to regulate the system frequency and also maintain the power exchanges between several control areas. The control center gathers the relevant frequency and power-flow information from across the control area and sends the appropriate set point adjustments for each of the

governor units in the AGC control loop. This AGC control is a slow control system where the wide-area control adjustments are changed every 15 to 30 seconds or so.

The wide-area controls for the voltage control called Secondary Voltage Control schemes are proposed in [13-17]. These papers present control schemes designed to manage voltage and reactive power on a wide network area. The main objective of the secondary voltage control is to adjust and to maintain the voltage profile inside a network area. Another objective is the control of reactive generation and flows. This type of control includes the modification of the set-point values of Automatic Voltage Regulation (AVR), the switching of compensation devices, and the change of tap position on transformers. The voltages of key buses are monitored and the control voltage set-points are sent to the local voltage controllers. New approaches for automatic voltage control was proposed in [18] that was motivated toward implementation in the transmission network operated by the Bonneville Power Administration (BPA) in the Pacific Northwest. Again, the secondary voltage control is also a slow control system with time constants ranging from 30 seconds to several minutes.

Advanced protection schemes called Special Protection Schemes (SPS's) or Remedial Action Schemes (RAS's) have also been developed in recent years. These schemes are designed to detect abnormal system conditions such as simultaneous loss of multiple transmission lines and to take predetermined corrective action to prevent the system wide instability. RAS schemes involve actions such as generation tripping, load shedding, capacitor insertion or transformer tap blocking, which are enforced at remote substations away from the fault location or other events. The use of SPS/RAS can increase the stability of power systems, especially for specific multiple line openings and

severe situations if they are designed properly. But these schemes are not flexible, since they require dedicated communication links and extensive offline calculations. In [19], a method for an adaptive RAS was proposed. The method calculates the difference of potential energy to determine each RAS action to increase the stability of the system, based on the transient energy analysis.

Most of current algorithms used in wide-area control are based on measurements of bus voltages and generator reactive power. Actually, it will be more effective to use the phase angle measurements to detect the angle instability, especially, the first swing instability in power systems [20]. Fast exchange of Phasor Measurements Units (PMU) among West Electricity Coordination Control (WECC) utilities is being pursued, and it is reasonable to assume the availability of system wide phase angle information (from specific PMU locations) in the near future [21]. This thesis proposes new algorithms that detect and mitigate transient instability by utilizing the phase angle measurements and frequency measurements of critical generator bus high side voltages from across the entire power system.

The main contributions of this thesis are listed as follows:

(1) A new algorithm based on the concept of the wide-area control using the phase angle measurements is proposed and the algorithm is tested in small standard test power systems. General conclusions drawn from the test systems will be helpful to study the larger power system.

(2) Extending the first algorithm, the idea of using approximate energy functions to detect the system instability in a real-time environment is carried out. The second algorithm is also tested in the two area system and the 39 bus test system.

All the simulations mentioned in this thesis are done using the Transient Security Assessment Tool (TSAT). TSAT is a software tool jointly developed by Powertech Labs Inc. and Nanjing Automation Institute.

The thesis is organized as follows. The algorithm using the system wide phase angles is described in Chapter 2, and the simulation results are also illustrated in this chapter. In Chapter 3, the second algorithm using the concept of real-time energy function is introduced together with the simulation results. The two algorithms are compared and analyzed in Chapter 4. In the last chapter, conclusions of this thesis are drawn and some future work is suggested.

CHAPTER 2 ALGORITHM USING THE PHASE ANGLE

2.1 INTRODUCTION

A first version of the phase angle based algorithm was postulated in Appendix 3 of the recent paper [21]. This chapter will discusses the new algorithm in more detail along with illustrative examples on standard IEEE test systems. These algorithms thus extend the framework of Wide-Area Control Systems (WACS) controller previously developed at Bonneville Power Administration and Washington State University by including phase angles into the algorithm computations.

2.2 ALGORITHM

The proposed algorithm extends the concept of the voltage-based algorithm Vmag from [21] into consideration of the phase angle measurements. At present, the algorithm analyzes the phase angles in two stages: 1) the angle stability within each control area, and 2) the angle stability of the entire large system. The principle in each step is similar.

First, let us recall the definition of the Center of Angles (COA) [5],

$$\delta_{COA} = \frac{\sum_{i=1}^{N} \bar{\delta}_i H_i}{\sum_{i=1}^{N} H_i} \tag{2.1}$$

where $\bar{\delta}_i$ is the internal machine rotor angle and H_i is the respective generator inertia time constant. Since the internal machine rotor angle can not be directly measured, we approximate the internal angle with the phase angle of the high side bus voltage which is normally monitored by synchrophasors. Similarly, the inertia time constant H_i in (2.1) is difficult to access in real-time. Therefore, we substitute the weights defined by the

inertia constants in (2.1) with the high side active power injections for the generators. The machine inertias are typically proportional to the real power outputs. The modified formula (2.2) presented below is thus readily suited for real-time computation using synchrophasors of PMU.

Let us assume the availability of the phase angle measurements, say, δ_j^i, from a few key generating plants, say for $j = 1, 2, ..., N$ in area i. Then, we introduce the notion of the approximate center of inertia angle reference for the area, say, δ_c^i, by the rule,

$$\delta_c^i = \frac{\sum_{j=1}^{N} \delta_j^i P_j^i}{\sum_{j=1}^{N} P_j^i} \tag{2.2}$$

where P_j^i denotes the current MW generation schedule at the plant j in area i. By increasing the number of angle measurements within each area, we can improve the accuracy of the computation of the angle reference δ_c^i and we can also improve the redundancy. Similarly, the center of inertia angle reference for the entire system, denoted δ_c, can be computed with the rule,

$$\delta_c = \frac{\sum_{i=1}^{N} \delta_c^i P^i}{\sum_{i=1}^{N} P^i} \tag{2.3}$$

where N is the total number of areas that are available in the control formulation, and P^i denotes the current total generation in Area i.

Next, we present a heuristic rule for detecting angle instability using these concepts in a real-time framework. When the representative angle δ_c^i of an area in (2.2) continuously increases away from the center of inertia δ_c beyond a pre–specified metric, we would heuristically interpret that Area i is moving towards separation from the rest of the system. In this case, a suitable remedial action could be the tripping of generation in that area. Similarly, when the angle δ_c^i continues to decrease beyond a predefined threshold, we would interpret that as a likely separation of Area i that could be countered by load shedding in Area i. There rules need to be crosschecked by analyzing the respective frequency measurements.

In our studies, we set the control trigger heuristics to be similar to the voltage error algorithm Vmag [21]. In the case of phase angles, we define $\Delta\delta_c^i = \delta_c^i - \delta_c$. We then accumulate two integral terms, denoted Ω_a^i and Ω_d^i, respectively, to denote the speeding up or slowing down of Area i with respect to the center of inertia reference frame. First, the term Ω_a^i is the integral for $\Delta\delta_c^i$, whenever $\Delta\delta_c^i$ continuously stays above a threshold, say $\Delta\delta_c^{i*}$. The accumulated error Ω_a^i is reset to zero whenever the angle $\Delta\delta_c^i$ drifts below $\Delta\delta_a^{i*}$. When Ω_a^i grows above a pre-specified value, say Ω_a^{i*}, the Area i is interpreted to be speeding away from the rest of the system and a suitable generation tripping may be initiated in that area. The value of Ω_a^{i*} will be tuned in real-time based on the current total generation and the current spinning reserve in Area i. That is, the smaller the current spinning reserve (relative to the total generation) in Area i, then the

lower the threshold value for Ω_a^{i*} . The computation of the Ω_d^i is then similar to accumulating the integral of $\Delta\delta_c^i$ below a threshold, denoted $\Delta\delta_d^{i*}$. When Ω_d^i grows above a pre-specified value, say Ω_d^{i*}, load shedding in Area i may be initiated to mitigate the disturbance event.

2.3 ILLUSTRATION OF THE ALGORITHM USING THE TWO AREA SYSTEM

We implement the above algorithm in the two area system (the diagram of the two area system is shown in Appendix A). The system is simply divided into two areas with Gen 1 and Gen 2 in Area 1, Gen 3 and Gen 4 in Area 2, respectively. We define

$$\delta_c^1 = \frac{\delta_1^1 P_{G1} + \delta_1^2 P_{G2}}{P_{G1} + P_{G2}} \tag{2.4}$$

$$\delta_c^2 = \frac{\delta_2^{31} P_{G3} + \delta_2^4 P_{G4}}{P_{G3} + P_{G4}} \tag{2.5}$$

Where δ_1^1 , δ_1^2 , δ_2^3 , δ_2^4 are the phase angles of the bus voltage of the four generators, respectively. Also, we define

$$\delta_c = \frac{\delta_1^1 P_{G1} + \delta_1^2 P_{G2} + \delta_2^3 P_{G3} + \delta_2^4 P_{G4}}{P_{G1} + P_{G2} + P_{G3} + P_{G4}} \tag{2.6}$$

$$\Delta\delta_c^1 = \delta_c^1 - \delta_c \text{ , } \Delta\delta_c^2 = \delta_c^2 - \delta_c \tag{2.7}$$

When we apply a three phase fault at BUS 8 and after some certain time we clear the fault and remove three of the four lines between BUS 7 and BUS 8 at time 0.1 sec, the details of the simulation results are shown below. When the fault-on time is set to be 0.08 sec, 0.10 sec, and 0.11 sec, the curves of $\Delta\delta_c^1$ and $\Delta\delta_c^2$ are shown in Figure 2-1, Figure 2-2 and Figure 2-3, respectively. Figure 2-4 shows the curve of $\Delta\delta_c^1$ near 60 degrees.

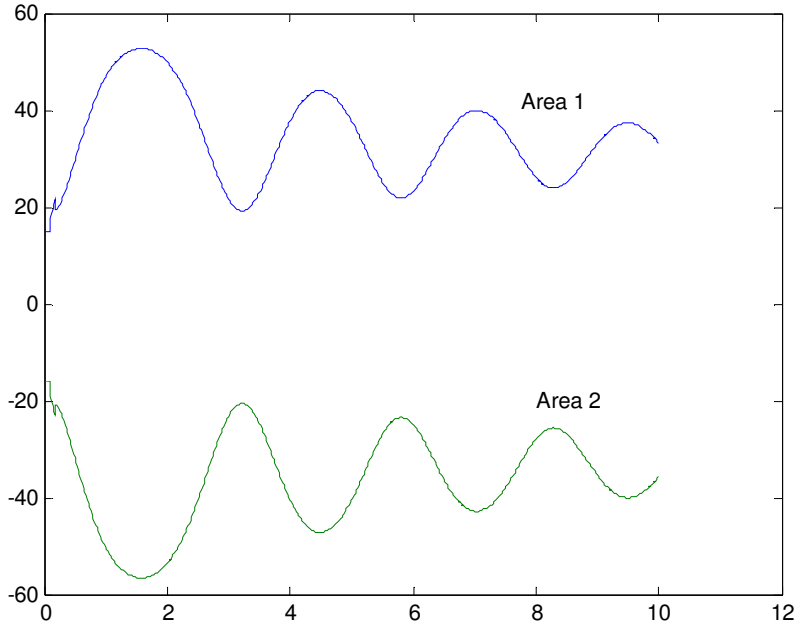

Figure 2-1 Angles of each area (fault-on time=0.08 sec)

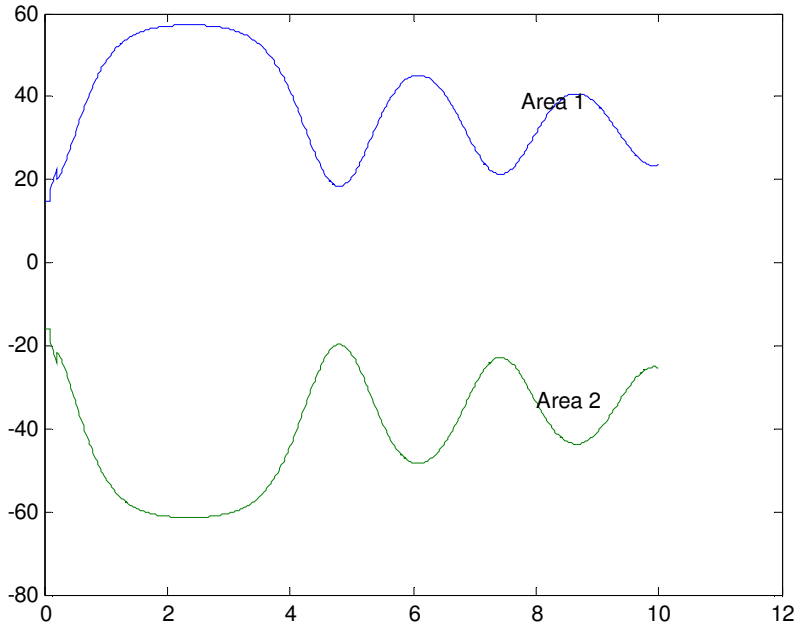

Figure 2-2 Angles of each area (fault-on time=0.10 sec)

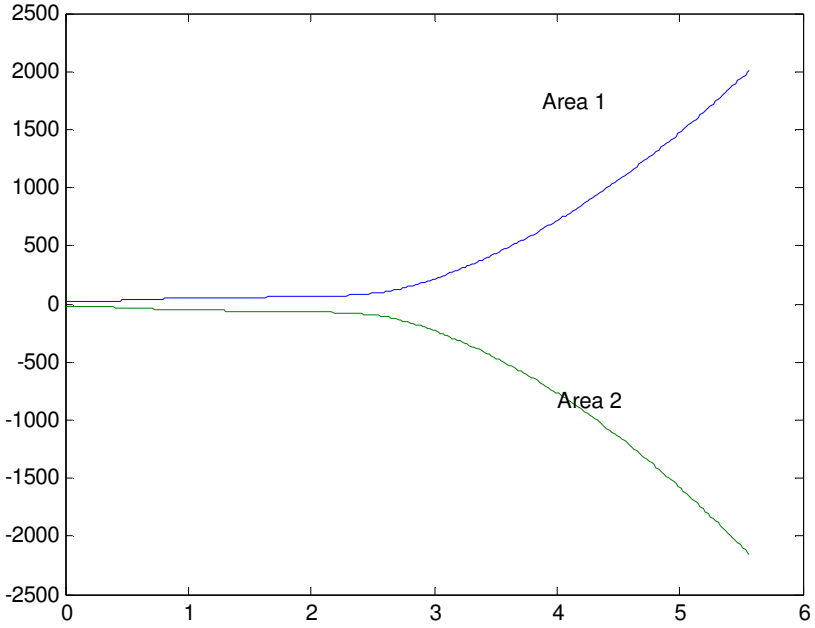

Figure 2-3 Angles of each area (fault-on time=0.11 sec)

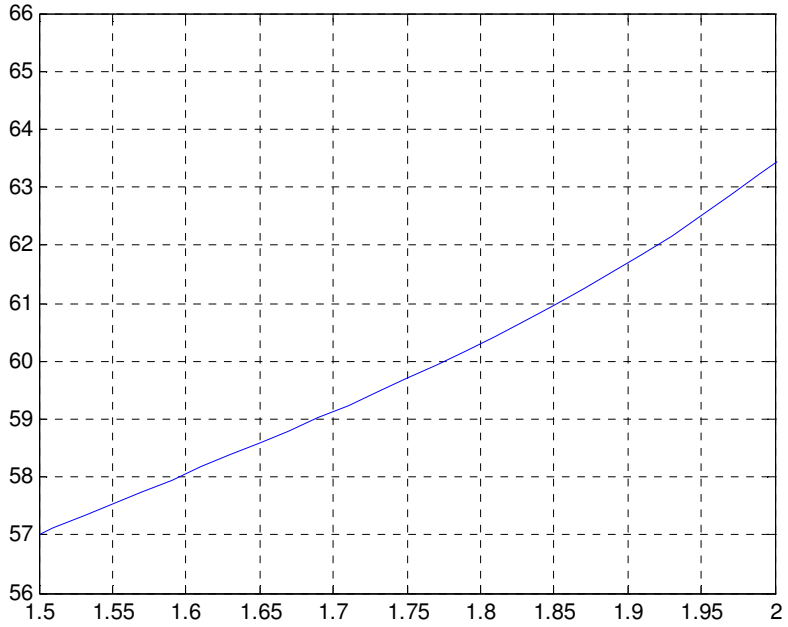

Figure 2-4 Angles of area 1 (fault-on time=0.11 sec)

From the cases above, we could say that 0.10 sec is the critical fault time for this three phase fault on Bus8. Looking into Figure 2-2, we could find that the maximum value of $\Delta\delta_c^1$ is 57.3 degrees and the minimum value of $\Delta\delta_c^2$ is -61.5 degrees. Therefore, we set $\Delta\delta_a^*$=60 degrees, $\Delta\delta_d^*$=-65 degrees, Ω_a^*=5 and Ω_d^*=-5. Simulation results with different fault-on time are shown in Table 2-1. From the results, we could say Area 1 is moving away from the system earlier than Area 2. When we try to trip some generation of Area 1, we find that the generation tripping action by itself is not enough to stabilize the system. Thus, we add some load shedding action in Area 2. We trip Gen 1 and 50% of the load at Bus 9 at time 1.83 sec for the second case in Table 2-1. The system can be stable as shown in Figure 2-5. Also, if we trip Gen 1 at time 1.83 sec and 50% load at Bus 9 at time 1.93 sec, the system can be stabilized as shown in Figure 2-6. As a result, the new algorithm works for this example in the two area system. Table 2-2 summarizes the benefits provided by the algorithm in improving the transient stability. Taking the first case as example, the critical clearing time without the proposed control is 0.10 seconds (the first entry in Table 2-1). The system becomes transient stable for the clearing time of 0.11 seconds as well as 0.12 seconds. With the automatic generation tripping control as proposed, the critical clearing time improves to 0.14 seconds. Compared to the 0.10 seconds for the original system with no control, the automatic controller as proposed provides an improved critical clearing time by a margin of 0.04 seconds (2.4 cycles).

Table 2-1 Simulation results for the two area system

Fault Time	0.10 sec	0.11 sec		0.12 sec	
Stability	Stable	Unstable		Unstable	
Area		Area1	Area2	Area1	Area2
T_start		1.73 sec	1.89 sec	1.52 sec	1.61sec

T_control		1.83 sec	1.93 sec	1.62 sec	1.69 sec
Int		6.0525	-5.2325	6.0965	-5.3345
T_unst		2.4 sec		2.0 sec	

*T_start is the time $\Delta\delta_a^1$ increases beyond $\Delta\delta_a^{1*}$; T_control is the time Ω_a^1 reaches Ω_a^{1*};

Int is the value of Ω_a^1 at T_control. T_unst is the time $\Delta\delta_c^1$ reaches 90 degrees.

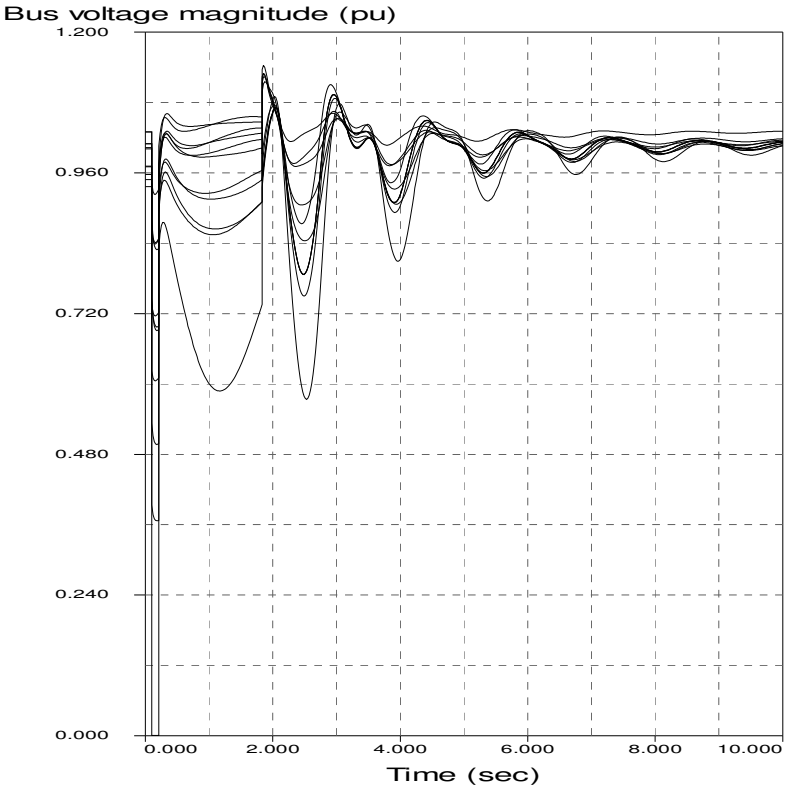

Figure 2-5 Bus voltages with tripping actions at same time (fault-on time=0.11 sec)

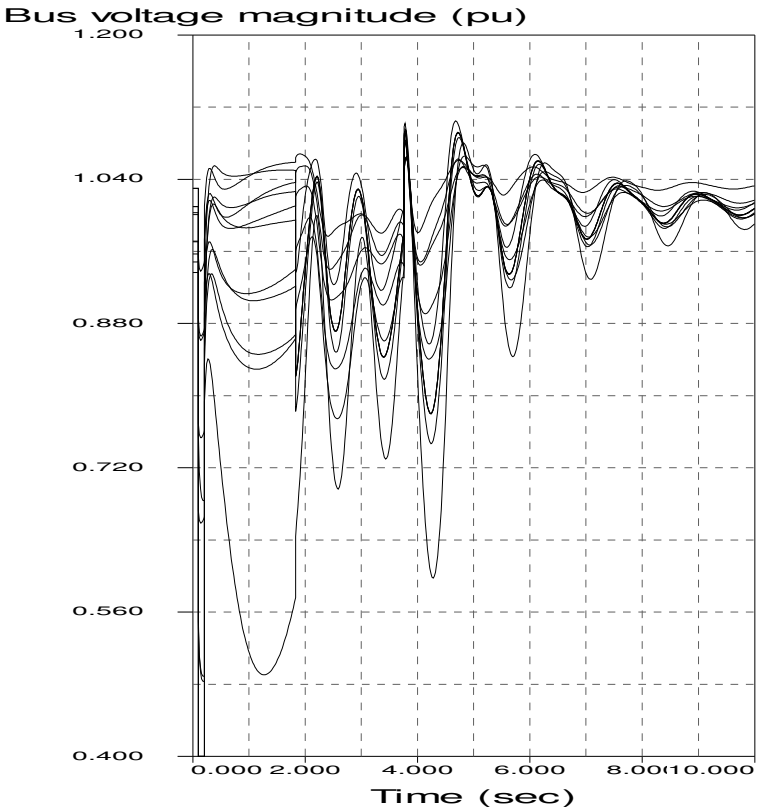

Figure 2-6 Bus voltages with tripping actions in turn (fault-on time=0.11 sec)

Table 2-2 Improvement on the system stability

Fault Bus	Line Removed	Fault Time (cycle) improvement
8	7-8	2.4
7	7-8	1.8

Tests in two area system lead to some discussions of the new algorithm.

(1) If we use inertia constants to compute δ_c as formula (2.1) shows, with the 0.11 sec-fault time, Figure 2-7 shows the comparison of the two methods. It shows that the substitution with power output to compute δ_c is reasonable.

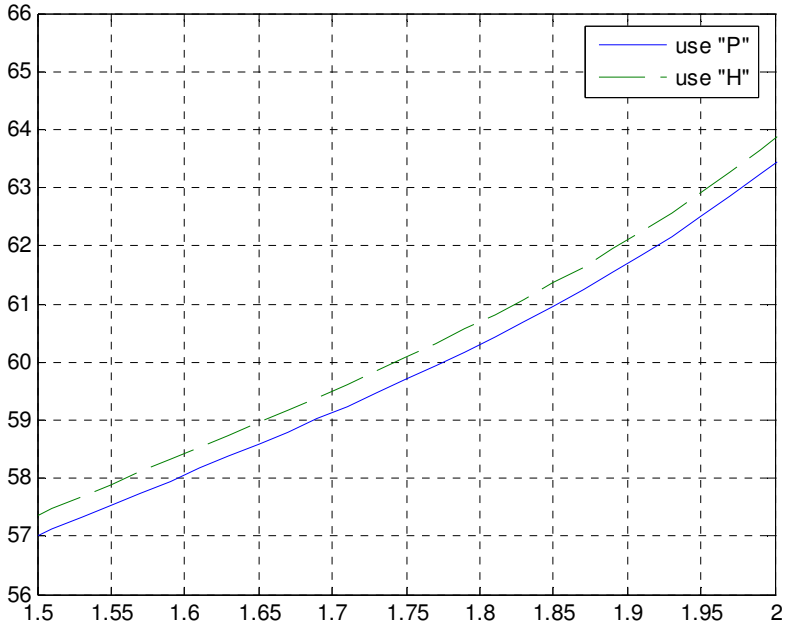

Figure 2-7 comparison of two ways to compute δ_c (fault-on time=0.11 sec)

(2) The thresholds are set up based on the critical cases and they need to be tuned in order to make the algorithm work reasonably for diverse conditions.

(3) Control actions such as the generation tripping in the accelerating area or load shedding in the decelerating area are the normal methods in system protection. But, the tripping or shedding amounts still need to be determined from further studies in future research works.

2.4 IMPLEMENTATION OF THE ALGORITHM IN THE 39 BUS SYSTEM

We also implement the algorithm in the 39 Bus System (the diagram of the 39 bus system is shown in Appendix B). In this system, we treat each generator bus is a individual control bus, thus, the algorithm is re-written as following:

1) The COA of the system is defined as,

$$\delta_c = \frac{\sum_{j=1}^{10} \delta_j P_j}{\sum_{j=1}^{10} P_j}$$, j is the number of the generator. (2.8)

2) In case of phase angles, we define $\Delta\delta_j = \delta_j - \delta_c$

3) The term Ω_a^j is the integral for $\Delta\delta_j$, whenever $\Delta\delta_j$ continuously stays above a threshold, say $\Delta\delta_a^*$. The accumulated error Ω_a^j is reset to zero whenever the angle $\Delta\delta_j$ drifts below $\Delta\delta_a^*$. When Ω_a^j grows above a pre-specified value sys Ω_a^*, the generator j is interpreted to be speeding away from the rest of the system and a suitable generation tripping may be initiated to that generator. The computation of the Ω_d^j is then similar to accumulating the integral of $\Delta\delta_j$ below a threshold, denoted $\Delta\delta_d^*$. When Ω_d^j grows above a pre-specified value , say Ω_d^*, load shedding in generator bus j may be initiated to mitigate the disturbance event, or, if the frequency of the generator j is above 60Hz, we need to trip this generator instead of load shedding.

4) In the 39 Bus System, $\Delta\delta_a^*$ is set to be 60 degrees, $\Delta\delta_d^*$ is set to be -70 degrees. These two thresholds are set up based on the observation of the boundary of phase angles in critical cases and the thresholds are also tested for most of routine the faults in the test system. The settings Ω_a^* and Ω_d^* are set to be 5 and -5 respectively.

Now, we introduce an example to explain the algorithm. There is a fault at Bus 4 and line 4-14 is removed after fault clearing. When the fault time is set to be 12 cycles, Figure 2-6 shows $\Delta\delta_j$ of each generator in the system and the system is classified to be stable. When the fault time is set to be 13 cycles, the Figure of phase angles is shown

below (Figure 2-7).

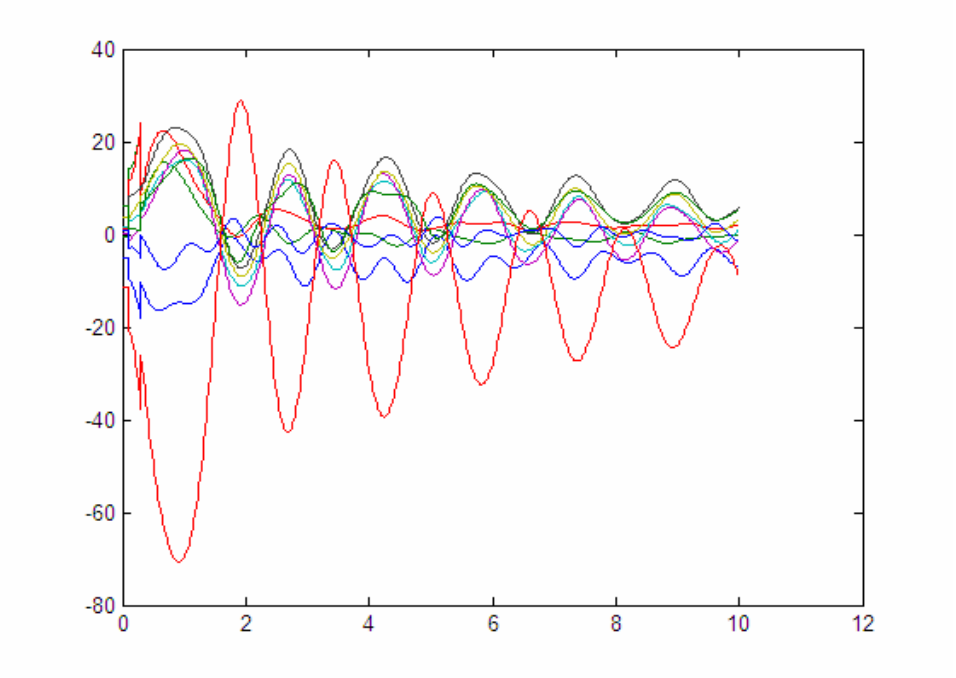

Figure 2-8 Angles of generators (fault-on time=12 cycles)

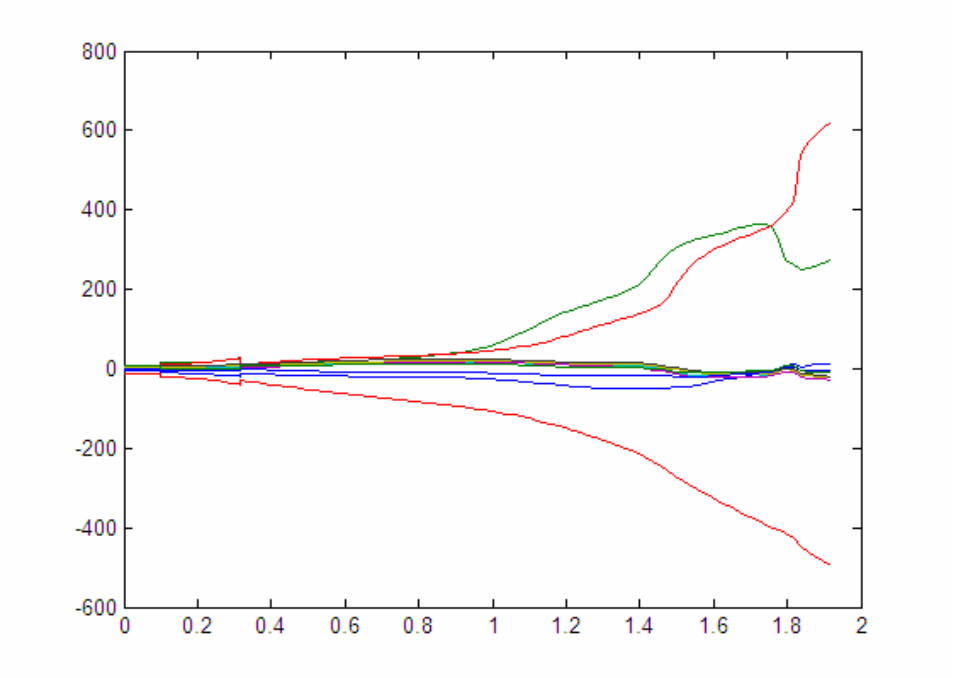

Figure 2-9 Angles of generators (fault-on time=13 cycles)

From the algorithm, generator 10 is the first to move away from the COA, the control time is 0.76 sec. So we trip Gen 10 to stabilize the system as the frequency of Gen 10 is above 60 Hz (Figure 2-7). The figure of the system bus voltages is shown below (Figure 2-8).

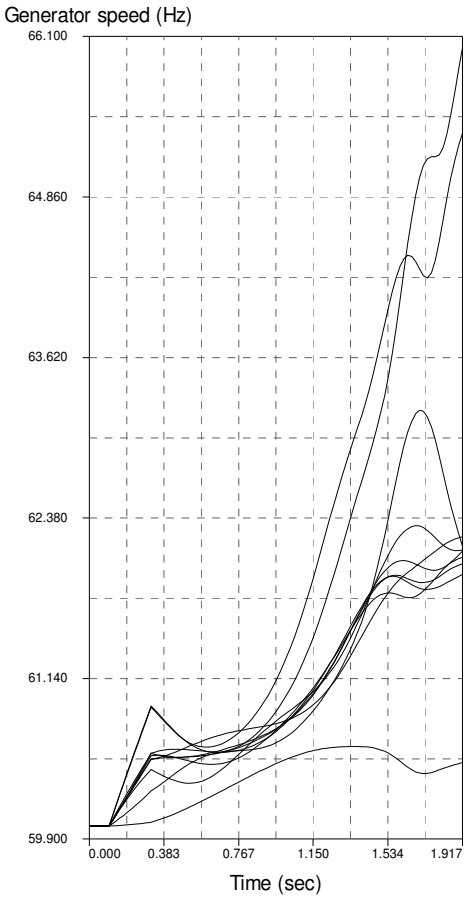

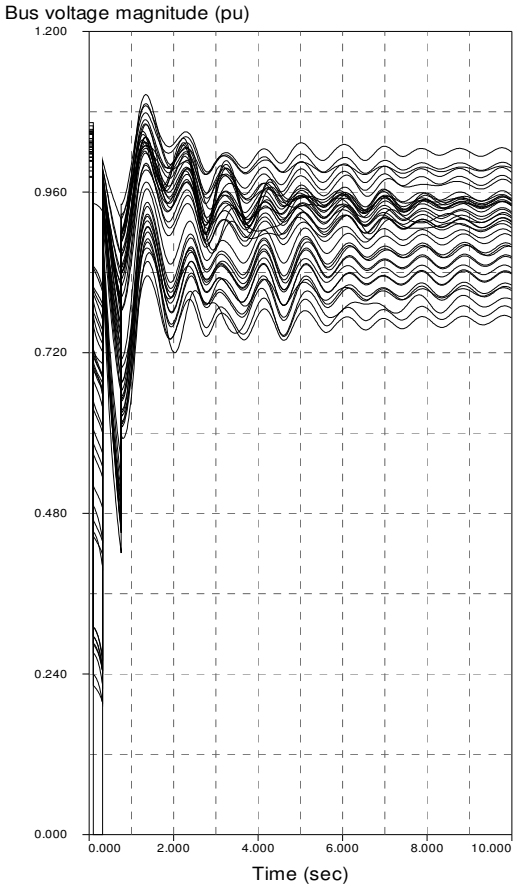

Figure 2-10 Generator speeds (fault-on time=13 cycles)

Figure 2-11 Bus voltages after tripping Generator 10 (fault-on time=13 cycles)

The following table (table 2-3) summarizes the simulation results for various single line outages. The fault time of each fault is the critical time when the system becomes unstable. The Gen tripped and tripping time is the generator needed to be tripped and the

tripping time that the algorithm initiates a control action. And after the generation tripping, the system will become stable.

Table 2-3 Simulation results for the 39 bus system

Fault Bus	Line Removed	Fault Time(cycles)	Gen tripped	tripping time(sec)
4	4-14	13	10	0.76
14	4-14	13	10	0.78
4	4-5	12	10	0.88
3	3-4	12	10	0.73
4	3-4	11	10	0.84
5	5-6	11	2	0.90
6	5-6	10	2	1.11
2	2-25	7	9	1.06
25	2-25	6	9	0.92
16	16-19	5	4,5	0.52
19	19-16	5	4,5	0.46
21	16-21	9	10	0.90
16	16-21	7	10	0.77

Table 2-4 Improvement on the system stability

Fault Bus	Line Removed	Fault Time(cycles) improvement
4	4-14	3
14	4-14	3
4	4-5	4
3	3-4	2
4	3-4	4
5	5-6	2
6	5-6	2
2	2-25	3
25	2-25	3
16	16-19	0
19	19-16	0
21	16-21	3
16	16-21	3

Table 2-4 summarizes the benefits provided by the algorithm in improving the

transient stability. For instance, let us consider the first contingency in Table 2-4, the three phase fault on Bus 4 and the loss of line 4-14. The critical clearing time without the proposed control is 12 cycles. For the 13 cycles-clearing time case, the phase angle based algorithm identifies Gen 10 as the critical generator and a trip signal is issued by the control to Gen 10 at 0.76 seconds (first entry of Table 2-3). Assuming that the generator is tripped by the proposed controller, the system becomes transient stable for the clearing time of 13 cycles as well as 14 cycles. With the automatic generation tripping control as proposed, the critical clearing time improves to 15 cycles. Compared to the 12 cycles for the original system with no control, the automatic controller as propose provides an improved critical clearing time by a margin of 3 cycles. Table 2-4 thus illustrates the effectiveness of the algorithm in detecting and mitigating transient stability contingencies in various parts of the system.

It is important to point out that the control decision is entirely based on the measured phase angles and the controller does not know what outage resulted in the observed phase angle responses. This is a purely response based algorithm in the spirit of the previous algorithms in [21].

From Table 2-4, the controller based only on phase angle improves the system security for all excepting two outages. For the two exceptions, the controller does not cause negative margins or effects. Thus, the controller does appear to be effective for the 39 bus system.

2.5 CONCLUSION

This chapter presents the algorithm for processing of phase angle measurements from across the system to decide whether any part or control area within the system is speeding away from the rest. When the angle separations go above preset thresholds, remedial actions such as generation and load tripping are ordered by the stability controller to keep the areas in synchronism. This new algorithm can detect and mitigate transient instability by utilizing the phase angle measurements of critical generator bus voltages. The algorithm can be realized in the simulation of the two area system and the 39 bus System. The thresholds are set up based on the critical cases and tuned in order to make the algorithm work for the whole system. Control actions such as Tripping generation in accelerating area or shedding load in decelerating area are the normal methods in system protection. But, if the frequencies of the generators in decelerating area are above 60Hz, we need to trip generation in this area instead of load shedding. The tripping or shedding amounts still need further studies in future research work.

CHAPTER 3 ALGORITHM USING THE ENERGY FUNCTION

3.1 BACKGROUND

Transient energy methods are mathematical techniques for analyzing the power system dynamics due to excursions in voltage phase angles and their magnitudes. The energy associated with the deviation from system equilibrium point is quantified as a kinetic energy function (KE) that is related to changes in rotor speeds and a potential energy function (PE) that is connected with changes in relative rotor phase angles. In our research, we are trying to establish the relation between the system transient behavior and the measurements from PMU. The transient energy method is used to analyze the system stability so that PMU based measurements can be used for detecting the system instability in real-time, and for activating suitable control actions.

Figure 3-1 illustrates the equal area stability criterion for "first swing" stability [20]. If the decelerating area (energy) above the mechanical power load line is greater than the accelerating area below the load line, stability can be maintained.

Transient energy analysis has been developed with substantial advances in recent years. The method to evaluate the transient response of a power system following a large disturbance was proposed in [24]. [25], [26]. [27] used energy functions to quantify the energy of a system disturbance. In 1982, Vitta1 [28] introduced the idea of an individual machine's energy function, and in 1988 Stanton used transient energy functions of an individual generator, to assess instability of individual sites [29-31]. The Energy Functions are fully described in references [26],[28],[30] and [31]. The algorithm using energy function to detect system instability based on PMU can be found in [32], where the definition of critical energy was carried out as criterion of system stability.

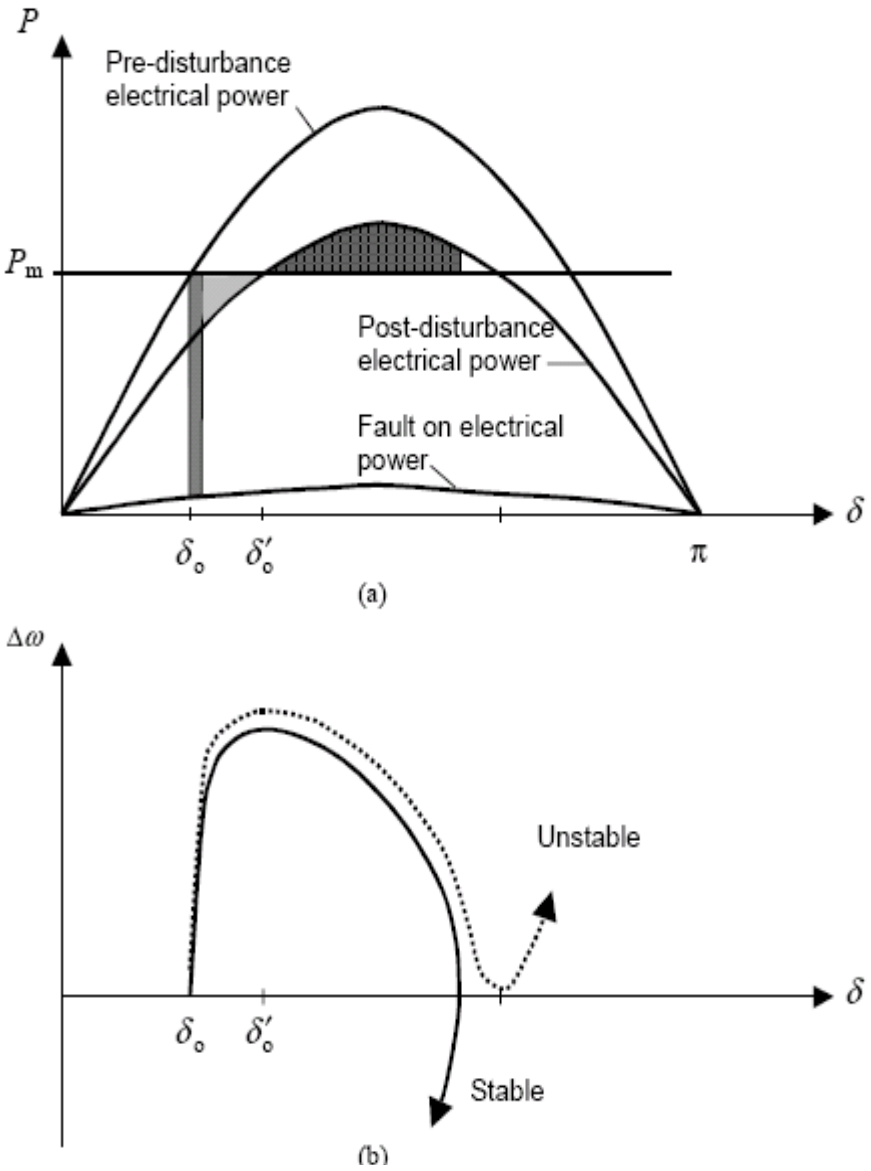

Figure 3-1 Angle stability illustration [20]
(a) Power angle curve and equal area criterion. Dark shading for acceleration energy during fault. Light shading for additional acceleration energy because of line outage. Black shading for deceleration energy. (b) Angle–speed phase plane. Dotted trajectory is for unstable case.

With the energy function analysis, it is possible to compute the swing energy associated with the system disturbances in simulation. Also, with the voltage phasor measurements date from PMU, it is possible to determine the swing energy in real time. Thus, the angle separation across the system can be monitored and control actions can be

taken to stabilize the system. In [32], the critical energy of each generator in the system is predetermined by the off-line computations. In real-time simulation, the computation of the kinetic energy function of each generator is used to detect whether the generators are remain in boundary in order to analyze the system stability. The recent paper [33] proposed a synchronous phasor data based energy function analysis in typical power transfer path with two generators. In our research, we carry out the potential energy function together with the kinetic energy function to define the total energy of each generator in the system. Computation of both energy functions in real-time is used to detect the system instability for the large power system with no restrictions on the size of the system or on the number of generators.

3.2 ALGORITHM

A Partial Energy Function is one that computes the transient energy of a single generator (or subsystem) in a multimachine system. In Partial Energy Function analysis, the transient energy for generator i, is defined as the integral of the power accelerating the generator's rotor,

$$PE_i = \int_{\theta_i} (PT_i - PG_i) \tag{3.1}$$

Transient energy can be resolved into Kinetic Energy, by

$$KE_i = H_i(\omega_i - 1)^2 \tag{3.2}$$

where ,

ω_i = rotor speed of generator

H_i = Inertia constant of generator

PT_i = torque

PG_i = MW generation of generator

θ_i =rotor angle

In our approach, we propose the real-time synchronous total energy of each generator in the system as the criterion to analyze the stability of the system. We define the total energy of each generator as TE_i,

where, $TE_i = KE_i + PE_i$. (3.3)

Now, we simply use TE_i to analyze the stability of the system by observing whether TE_i are remaining bounded. In practice, it is not convenient to get measurements of the rotor speed or angle. $\tilde{\omega}_i$ and $\tilde{\theta}_i$, representing the generator high side bus frequency and voltage angle, respectively, are introduced into the simulation.

3.3 ILLUSTRATION OF THE ALGORITHM IN THE TWO AREA SYSTEM

In the two area system, when we apply a three phase fault at BUS 8 and after some certain time we clear the fault and remove three of the four lines between BUS 7 and BUS 8 at time 0.1 sec, the details of the simulation results are shown below.

With the fault-on time 10 cycles, potential energy, kinetic energy, and total energy of each generator are shown in Figure 3-2, Figure 3-3 and Figure 3-4, respectively.

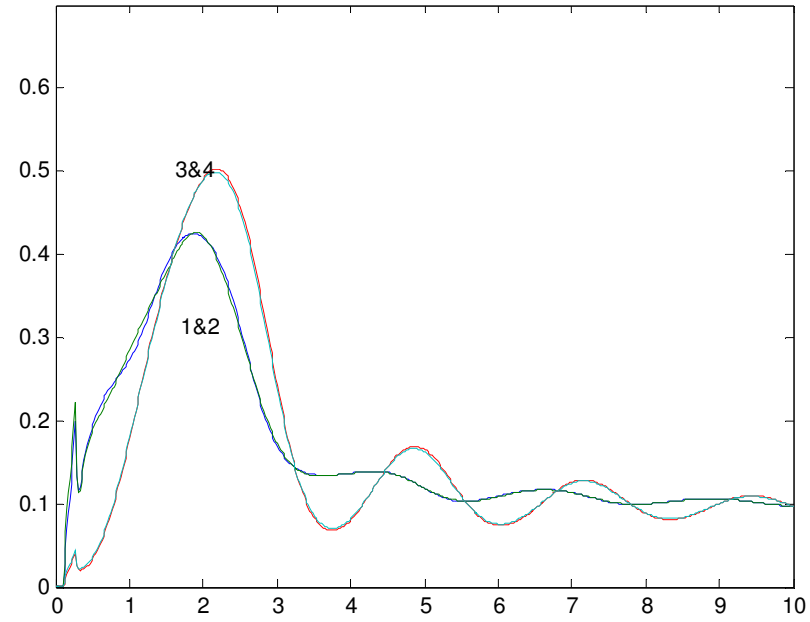

Figure 3-2 Kinetic energy of each generator (fault-on time=10 cycles)

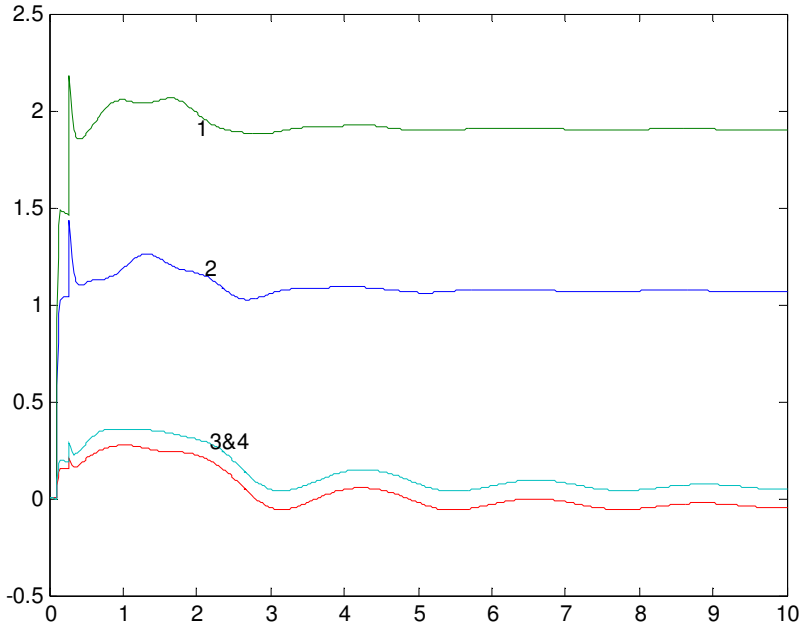

Figure 3-3 Potential energy of each generator (fault-on time=10 cycles)

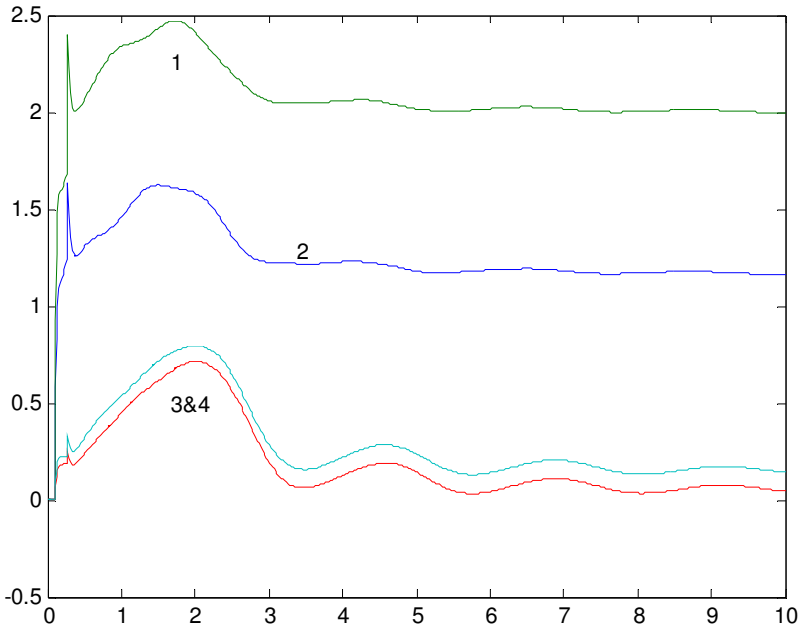

Figure 3-4 Total energy of each generator (fault-on time=10 cycles)

With the fault-on time 11 cycles, potential energy, kinetic energy, and total energy of each generator are shown in Figure 3-5, Figure 3-6 and Figure 3-7, respectively. If we put different thresholds for the four generators, we could implement some controls when the system goes unstable. For example, we set the thresholds as [2.0, 2.7, 1.0, 1.0], the time of each generator moving above thresholds is [1.68 sec, 1.52 sec, 9.68 sec, 9.56 sec], thus we can take some certain control to generator 1 to stabilize the system.

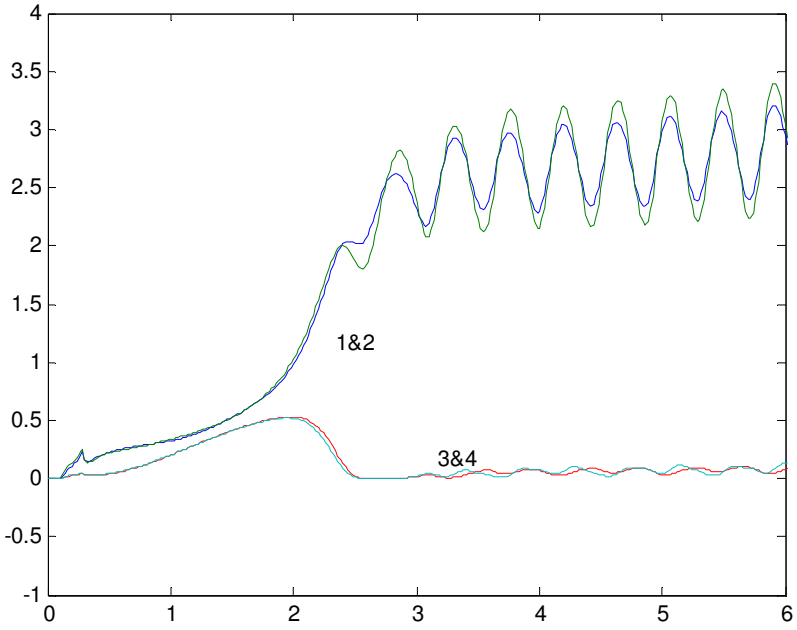

Figure 3-5 Kinetic energy of each generator (fault-on time=11 cycles)

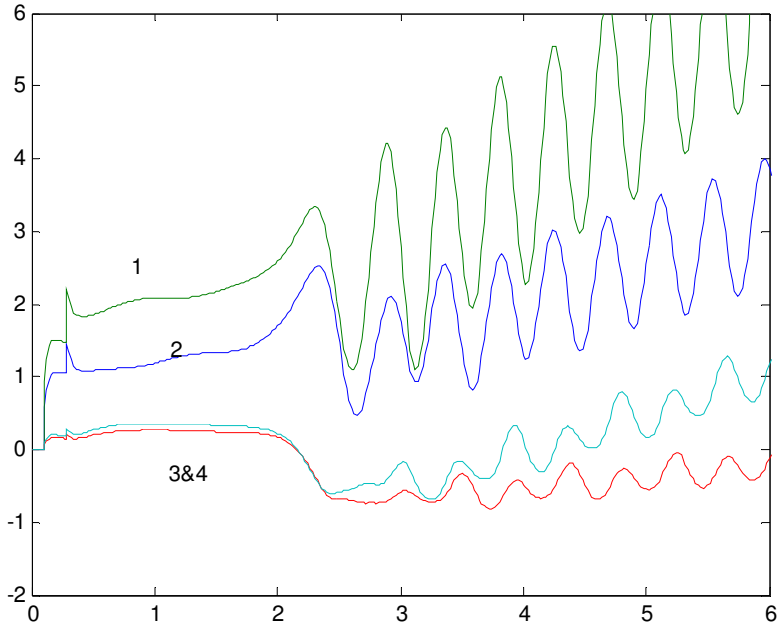

Figure 3-6 Potential energy of each generator (fault-on time=11 cycles)

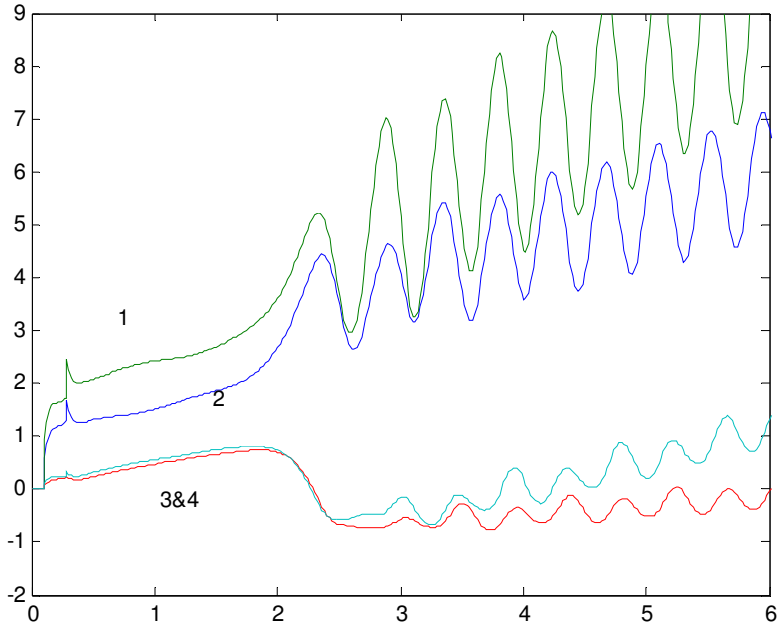

Figure 3-7 Total energy of each generator (fault-on time=11 cycles)

From the simulation results, it can be observed that the energy of each generator remains bounded in the stable cases and increases fast in the unstable cases. Thus, the energy function can be used as the criterion to analyze the stability of power system.

Now, we set the thresholds for the four generators as [2.0, 2.7, 1.0, 1.0], the simulation results with different fault-on time are shown in Table 3-1. Gen 2 is the first generator to move above the energy bound. Tripping Gen 2 and shedding 50% load of Area 2 at time 1.52 sec will stabilize the system. Table 3-2 lists the results that the algorithm improves the system stability.

Table 3-1 Simulation results for the two area system

	10cycles	11cycles	12cycles	13cycles
Stability	Stable	Unstable	Unstable	Unstable
Critical Gen		2	2	2
T_control		1.52 sec	1.37 sec	1.21 sec

Table 3-2 Improvement on the system stability

Fault Bus	Line Removed	Fault Time(cycles) improvement
8	7-8	3
7	7-8	2

3.4 IMPLEMENTATION OF THE ALGORITHM IN THE 39 BUS SYSTEM

We also implement the algorithm in the 39 bus System. Now, we introduce an example to explain the algorithm. There is a fault at Bus 4 and line 4-14 is removed after fault clearing. With the fault-on time 12 cycles, potential energy, kinetic energy, and total energy of each generator are shown in Figure 3-8, Figure 3-9 and Figure 3-10, respectively. With the fault-on time 13 cycles, potential energy, kinetic energy, and total energy of each generator are shown in Figure 3-11, Figure 3-12 and Figure 3-13, respectively. Therefore, if we put different thresholds to the generators, we could implement some controls when the system goes unstable.

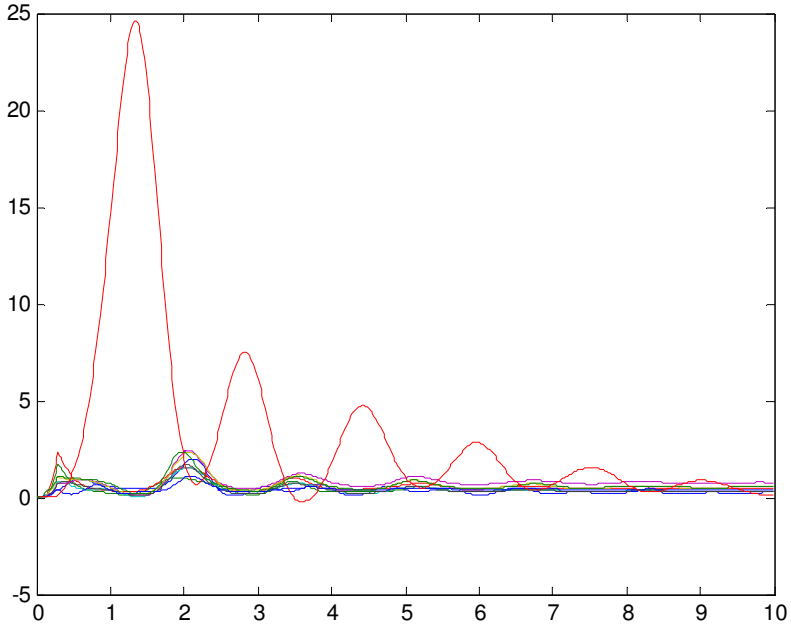

Figure 3-8 Potential energy of each generator (fault-on time=12 cycles)

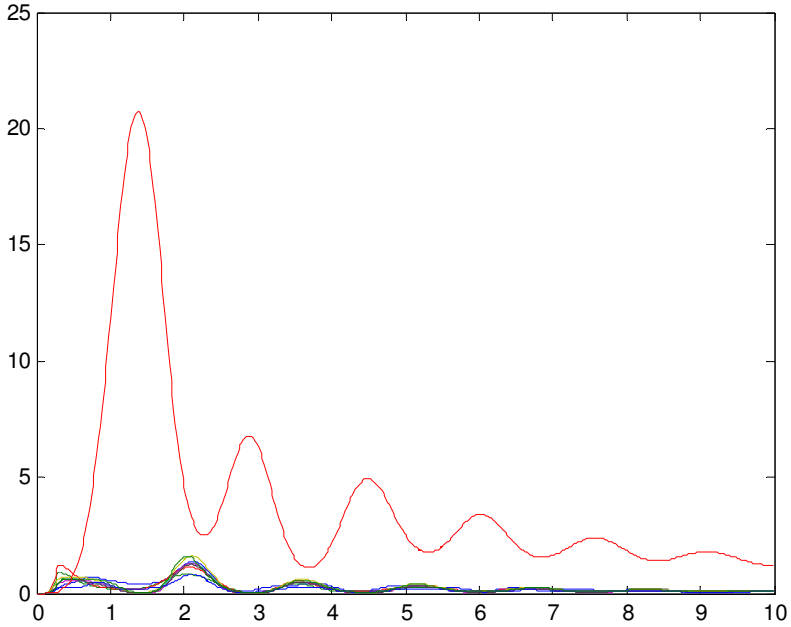

Figure 3-9 Kinetic energy of each generator (fault-on time=12 cycles)

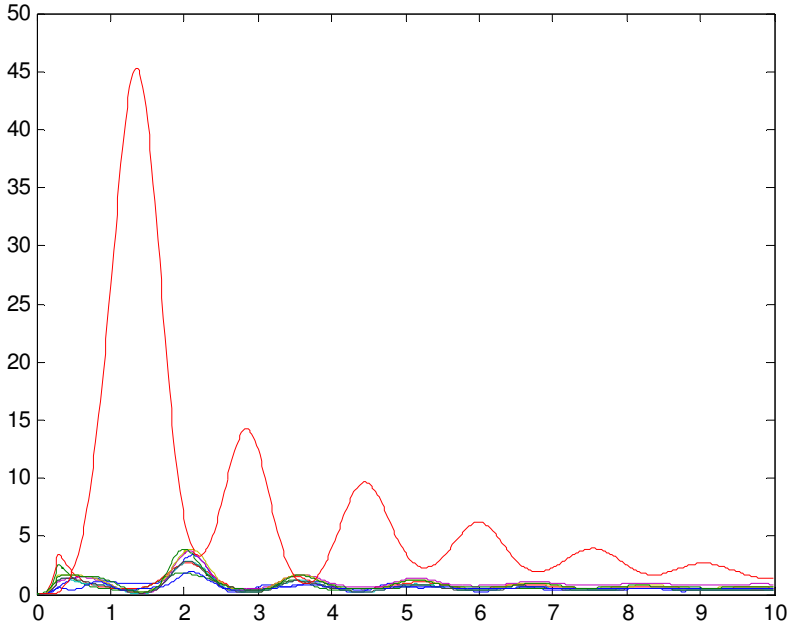

Figure 3-10 Total energy of each generator (fault-on time=12 cycles)

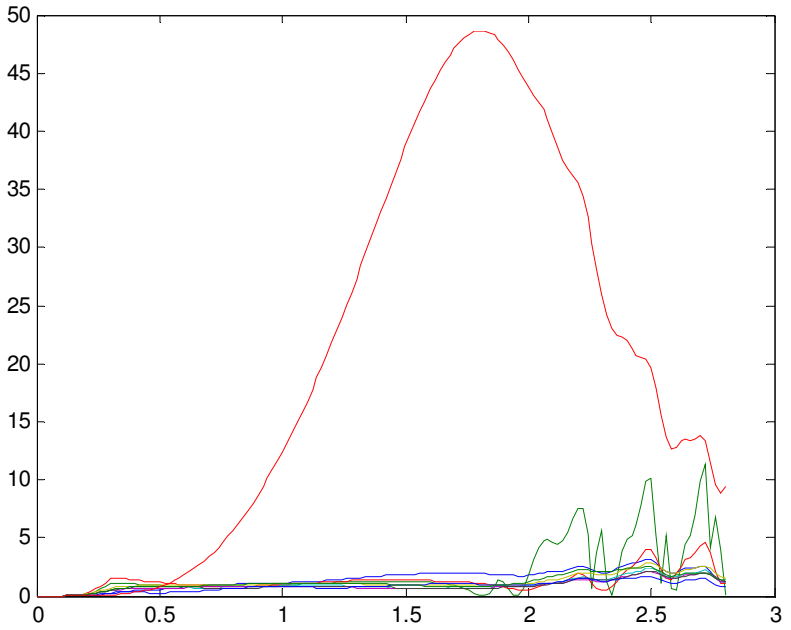

Figure 3-11 Potential energy of each generator (fault-on time=13 cycles)

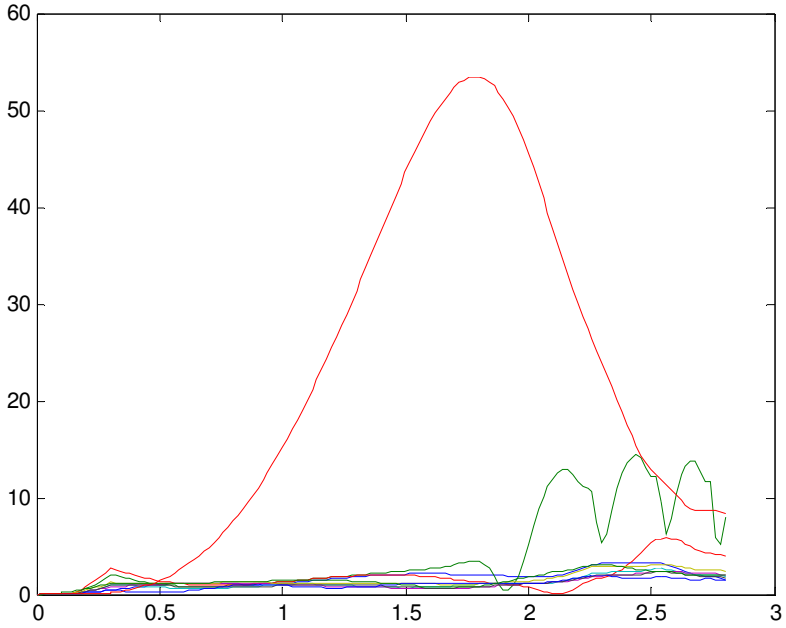

Figure 3-12 Kinetic energy of each generator (fault-on time=13 cycles)

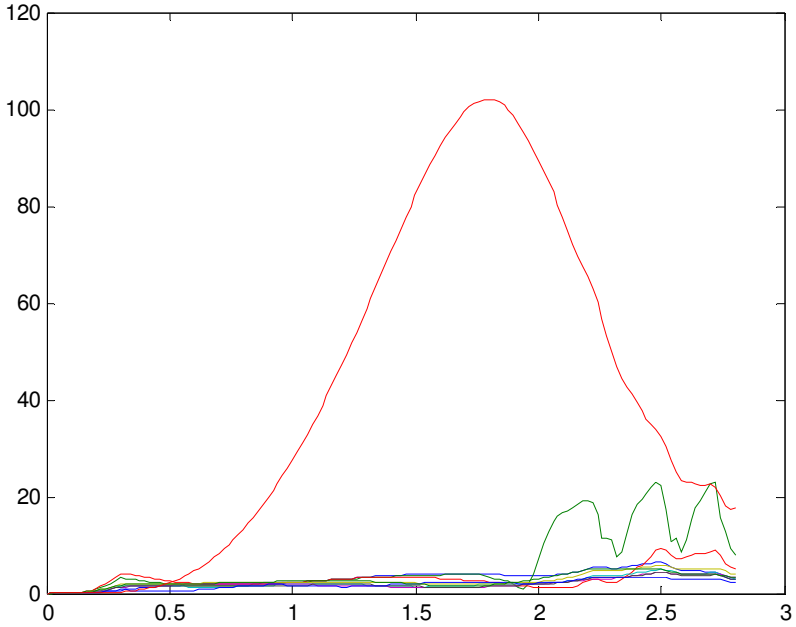

Figure 3-13 Total energy of each generator (fault-on time=13 cycles)

Since Gen 10 is much larger compared to the rest generators in capacities, the energy bound also needs to be set larger than the rest. For example, we set 50 as the threshold for Gen 10, 10 for the rest generators. The following table (Table 3-3) shows the simulation results. The fault time of each fault is the critical time when the system becomes unstable. The Gen is the critical generator that the algorithm gives out. Table 3-4 lists the results that the algorithm improves the system stability. Considering the first contingency in Table 3-4, there is a three phase fault on Bus 4 and line 4-14 is removed after clearing. The critical clearing time without the proposed control is 12 cycles. For this case, the energy function based algorithm identifies Gen 10 as the critical generator and a trip signal is issued by the control to Gen 10 at 1.09 seconds. Assuming that the generator is tripped by the proposed controller, the system becomes transient stable for the clearing time of 13 cycles as well as 14 cycles. Compared to the 12 cycles for the original system with no control, the automatic controller as propose provides an improved critical clearing time by a margin of 2 cycles. Recalling Table 2-3 and Table 2-4, we could find the energy function based algorithm consumes more time in identifying system instability, so that the improvement is not as effective as the angle based algorithm.

Table 3-3 Simulation results for the 39 bus system

Fault Bus	Line Removed	Fault Time(cycles)	Gen tripped	tripping time(sec)
4	4-14	13	10	1.09
14	4-14	13	10	1.13
4	4-5	12	10	1.31
3	3-4	12	10	0.99
4	3-4	11	10	1.03
5	5-6	11	2	1.23
6	5-6	10	2	1.37
2	2-25	7	9	1.41

25	2-25	6	9	1.32
16	16-19	5	4,5	0.58
19	19-16	5	4,5	0.52
21	16-21	9	10	1.02
16	16-21	7	10	0.92

Table 3-4 Improvement on the system stability

Fault Bus	Line Removed	Fault Time(cycles) improvement
4	4-14	2
14	4-14	2
4	4-5	3
3	3-4	1
4	3-4	1
5	5-6	1
6	5-6	1
2	2-25	0
25	2-25	0
16	16-19	0
19	19-16	0
21	16-21	1
16	16-21	1

3.5 CONCLUSION

The work reported in this chapter investigated the ability of energy function based on synchronized phase angle measurements to identify impending instabilities. The definition of the potential energy and the kinetic energy carry out new concepts of energy analysis in real-time large power system control. The new algorithm is tested on both the two area system and the 39 bus system.

CHAPTER 4 TESTS USING VARIOUS SIMULATION CONDITIONS

In Chapter 2 and Chapter 3, the two algorithms were proposed and tested in both the two area system and the 39 bus system. In this Chapter, we discuss variations of the simulation conditions, load model and the comparison of the two algorithms are carried out and lead to some conclusions.

4.1 ALGORITHM USING THE PHASE ANGLES

4.1.1 Multiple contingencies

In Chapter 2, the simulation results are based on single three phase fault on buses. More simulations are listed below with different fault type and conditions.

(1) Results of the two area system

(a) When we apply a three phase fault at BUS 9 and after some certain time we clear the fault and remove one of the three lines between BUS 8 and BUS 9 at time 0.1 sec, the system will maintain stable even the fault-on time increases to 0.25 sec.

(b) When we remove two of the three lines between BUS 8 and BUS 9 at time 0.1 sec, the system will collapse as the simulation shows. The angle of Area 1 will reach the threshold at 0.92 sec, and the controller will identify the instability and send out a tripping signal at 1.00 sec. But since the fault is too severe, the control actions including generation tripping in Area1 and load shedding in Area 2 will not stabilize the system.

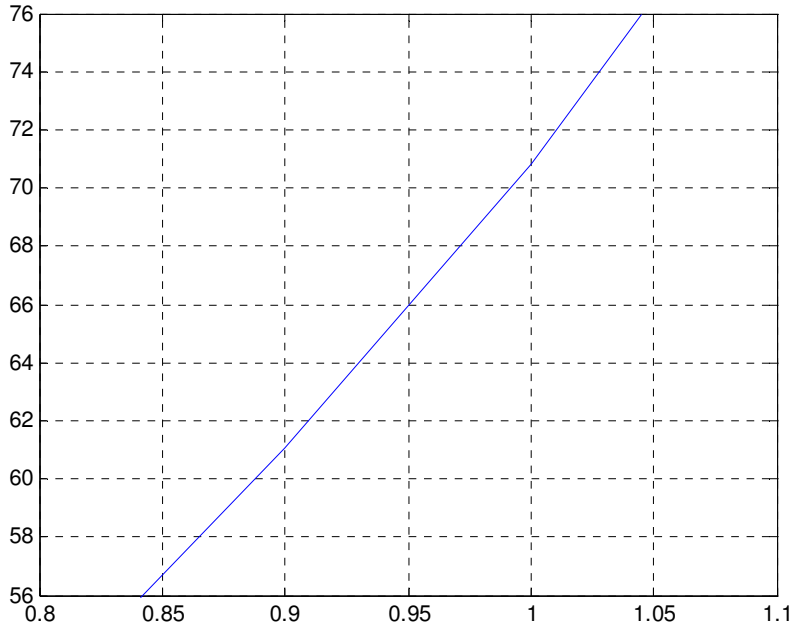

Figure 4-1 Angle of Area 1 when removing two lines between Bus 8 and Bus 9

(2) Results for the 39 bus system

Suppose there is a fault at Bus 4, line 4-14 and 3-4 are both removed after fault clearing. When the fault time is set to be 5 cycles, Figure 4-2 shows $\Delta\delta_j$ of each generator in the system. The algorithm gives out a stable result as the Figure 4-3 shows. When the fault time is set to be 6 cycles, the Figure of phase angles is shown below in Figure 4-4.

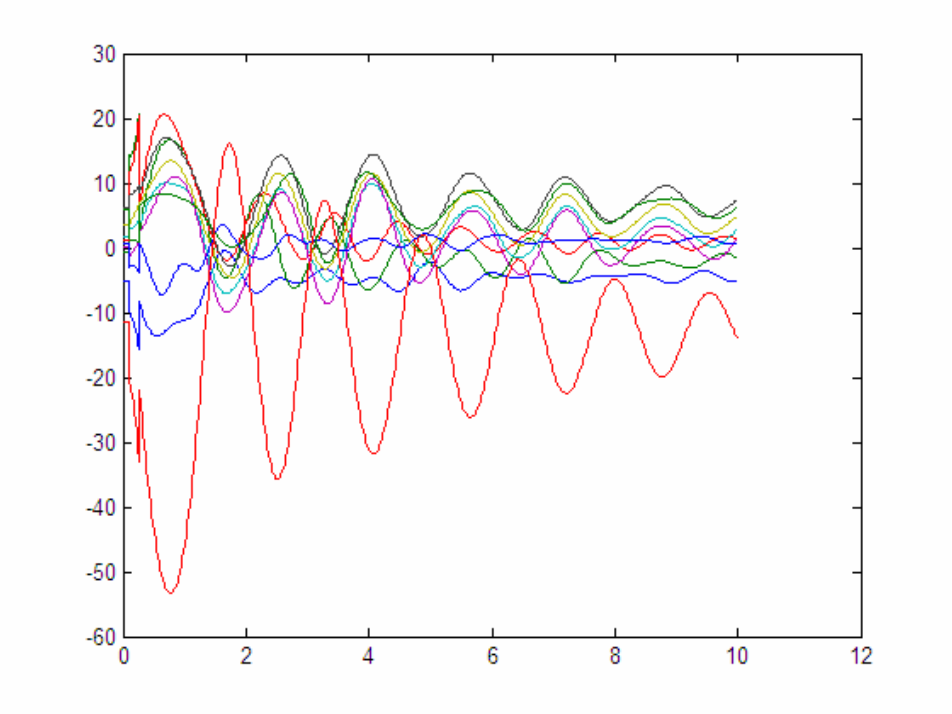

Figure 4-2 Angles of generators (fault-on time=5 cycles)

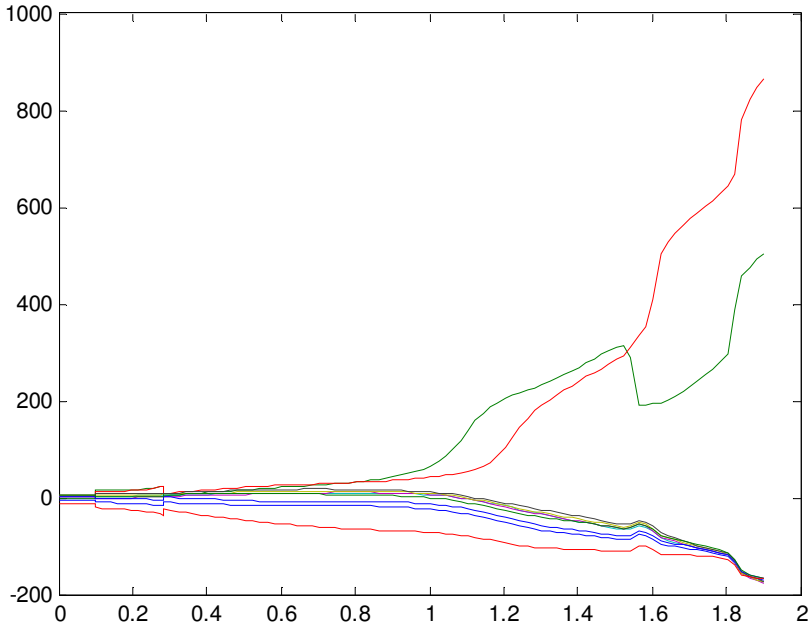

Figure 4-3 Angles of generators (fault-on time=6 cycles)

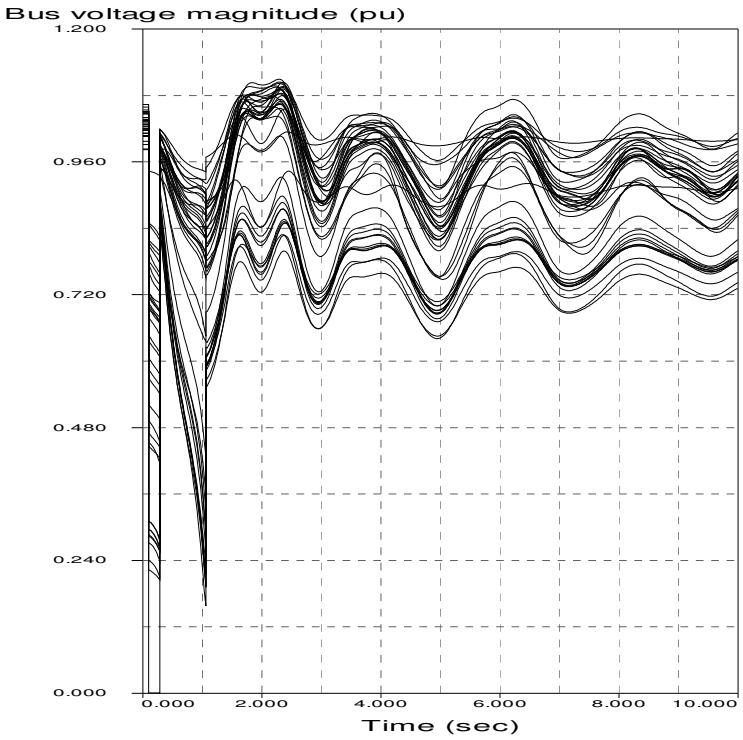

Figure 4-4 Bus voltages after tripping generator (fault-on time=6 cycles)

From the algorithm, generator 10 is the first to move away from the COA, the control time is 1.06 sec. So we trip Gen 10 to stabilize the system as the frequency of Gen 10 is above 60 Hz. The bus voltage Figure of the system is shown left in Figure 4-3. In this case, the critical clearing time will be improved by 2 cycles for the double contingency with the proposed angle based algorithm.

4.1.2 Consideration of the load level and the load model

(1) Results of the two area system

We decrease the load in the previous the two area system and get a new power-flow solution, then we simulate the same fault tested in Chapter 2, the results are shown in Table 4-1. In this case, when the clearing time is 0.20 seconds, the controller will

identify the system instability at time 1.38 second, a proper tripping generation in Area 1 will stabilize the system. And the improvement of clearing time is 1.8cycles.

Table 4-1 Simulation results for the two area system with different load

Clearing time	0.19 sec	0.20 sec	0.21 sec	0.22 sec
Stability	Stable	Unstable	Unstable	Unstable
T_start		1.28 sec	1.13 sec	1.04 sec
T_control		1.38 sec	1.23 sec	1.14 sec
Int		6.0986	6.1133	6.1330
T_unst		2.0 sec	1.75 sec	1.60 sec

(2) Results for the 39 bus system

(a) The previous 39 bus system is using a constant current load model. Now we change the load model to a ZIP model, which is 30% constant power, 30% constant current, 40% constant impedance, and we also add the typical governor to each generator. Table 4-2 shows the simulation results. The fault time of each fault is the critical time the system becomes unstable. The Gen tripped and tripping time is the generator needed to be tripped and the tripping time that the algorithm gives out. And after tripping generator, the system will become stable in each case. Table 4-3 lists the results that the algorithm improves the system stability. Since the system load is effectively decreased, the algorithm is more effective compared to Table 2-4.

Table 4-2 Simulation results for the 39 bus system with the different load model

Fault Bus	Line Removed	Fault Time(cycles)	Gen tripped	tripping time(sec)
4	4-14	12	10(50%)	0.86
14	4-14	12	10(50%)	0.88
4	4-5	11	10(50%)	0.98
3	3-4	12	10(50%)	0.84
4	3-4	12	10(50%)	0.93
5	5-6	11	2	0.97
6	5-6	10	2	1.19
2	2-25	7	9	1.12

25	2-25	6	9	0.98
16	16-19	5	4,5	0.54
19	19-16	5	4,5	0.50
21	16-21	10	10(50%)	0.97
16	16-21	8	10(50%)	0.79

Table 4-3 Improvement on the system stability

Fault Bus	Line Removed	Fault Time(cycles) improvement
4	4-14	5
14	4-14	5
4	4-5	4
3	3-4	3
4	3-4	4
5	5-6	2
6	5-6	2
2	2-25	4
25	2-25	4
16	16-19	0
19	19-16	0
21	16-21	3
16	16-21	3

(b) Continuing with the previous ZIP (30%, 30%, 40%) load model, we increase the load level to 120% and distribute the load to each generator of the system. Table 4-4 shows the simulation results. The fault time of each fault is the critical time the system becomes unstable. Since the system condition is severe, when the first phase angle moves above the pre-specified threshold, we take a generation tripping in accelerating area; at the same time, we also add load shedding action in decelerating area. In each unstable case, Gen 10 is the one which decelerates from COA, so we shed 50% load (600MW) at the Bus 39 which is the terminal bus of Gen 10 at the time the first angle moves beyond threshold. Table 4-5 lists the results that the algorithm improves the system stability. This test shows that the algorithm can still work with a stress system condition.

Table 4-4 Simulation results for the 39 bus system in a stress condition

Fault Bus	Line Removed	Fault Time(cycles)	Gen tripped	tripping time(sec)
4	4-14	7	2,3	0.87
14	4-14	7	2,3	0.86
4	4-5	6	2,3	0.93
3	3-4	7	2,3	0.85
4	3-4	7	2,3	0.95
5	5-6	6	2	0.99
6	5-6	5	2	1.06
2	2-25	6	9	1.05
25	2-25	5	9	0.89
16	16-19	5	4,5	0.53
19	19-16	5	4,5	0.51
21	16-21	7	2,3	0.93
16	16-21	6	2,3	0.81

Table 4-5 Improvement on the system stability

Fault Bus	Line Removed	Fault Time(cycles) improvement
4	4-14	0
14	4-14	0
4	4-5	1
3	3-4	1
4	3-4	2
5	5-6	1
6	5-6	1
2	2-25	2
25	2-25	2
16	16-19	0
19	19-16	0
21	16-21	1
16	16-21	1

4.1.3 Consideration of the communication time

In real-time control we need to consider the communication time of the control. Suppose the average communication time from PMU units to control center to be 0.075 sec. Thus, we take this time as 0.15 sec (a round-trip between PMU units and control

center) and resimulate the example in chapter 2 again. Therefore, the new control time is 0.91 sec. The algorithm will still stabilize the system as shown in Figure 4-5. As a result, the shorter time is consumed in communication, the more effective the algorithm will be (Table 4-6).

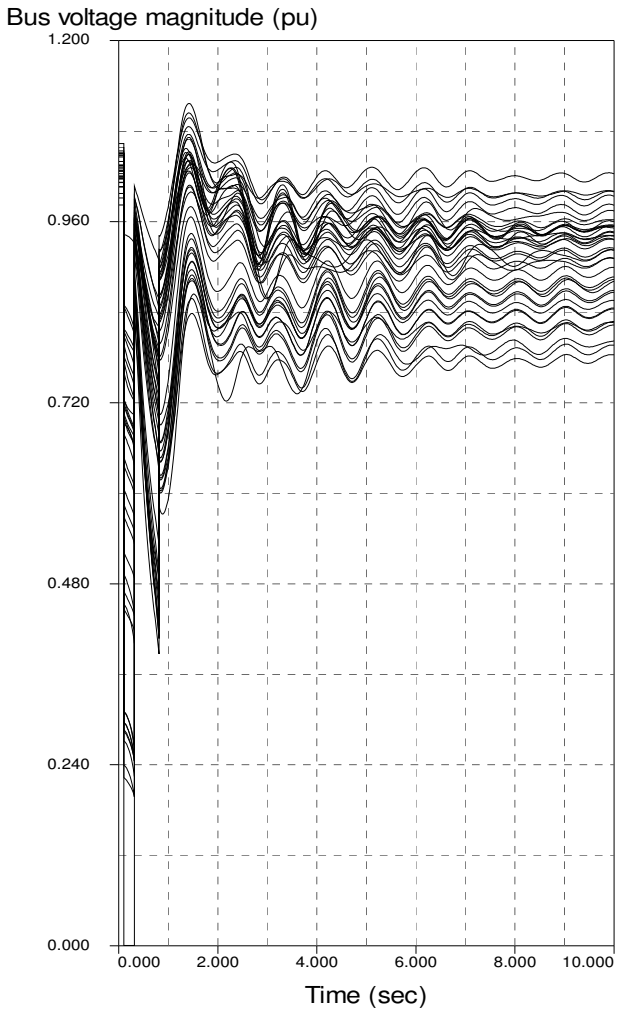

Figure 4-5 Bus voltages after tripping generator (communication time considered)

Table 4-6 Effects of communication time on system stability improvement

Communication time		0	0.10 sec	0.15 sec	0.20 sec
Improvement on the system stability (cycles)	Angle method	3	2	1	0
	Energy method	2	1	0	0

4.2 LOSS OF MEASUREMENTS

Now, we take the 39 bus system example with 13 cycles clearing time in chapter 2 and suppose the phase measurements of Bus 32 (not the critical one) are lost due to some reasons. The simulation result will still give out Gen 10 as the critical generator and the control time is 0.80 sec. Table 4-7 illustrates the results with the loss of measurements. With ten measurements from the 39 bus system, loss of one or two angle measurements will not lead to a large detecting error due to the weight average used in the computation of COA.

Table 4-7 Simulation results in case of Loss of measurements

Loss of measurement	No loss	Bus32	Bus30,32	Bus 30,32,35
Control time	0.76s	0.80 s	0.79 s	0.83 s
Critical Gen	Gen 10	Gen 10	Gen 10	Gen 10
Stability after control actions	Stable	Stable	Stable	Stable

4.3 ALGORITHM USING THE ENERGY FUNCTION

In section 4.1, we test the first algorithm with different simulation conditions. For the algorithm using the energy function, the same test could lead to similar results.

4.3.1 Multiple contingencies

(1) Results for the two area system

When we remove two of the three lines between BUS 8 and BUS 9 at time 0.1sec, the system will collapse as the simulation shows. The energy of Gen 1 and 2 will reach the threshold at 1.20 sec together (figure 4-6), and the controller will identify the instability and send out a tripping signal at 1.20 sec. But since the fault is too severe, the control actions including generation tripping and load shedding will not stabilize the system.

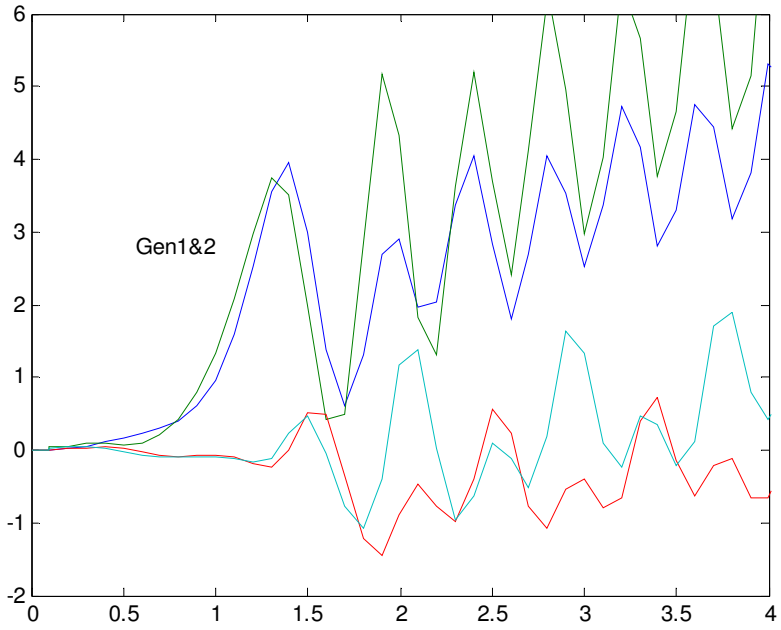

Figure 4-6 Total energy of each generator removing two lines between Bus 8 and Bus 9

(2) Results for the 39 bus system

Suppose there is a fault at Bus 4, line 4-14 and 3-4 are both removed after fault clearing. When the fault time is set to be 6 cycles, the system will collapse. From the algorithm, generator 10 is the first to move above the energy bound, the control time is 1.58 sec. So we trip Gen 10 to stabilize the system as the frequency of Gen 10 is above 60 Hz. In this case, the critical clearing time will be improved by 1 cycle with the proposed

energy function algorithm.

4.3.2 Consideration of the load level and the load model

(1) Results of the two area system

WE use the same system as shown in 4.1.2(1), the results are shown in Table 4-8. In this case, when the clearing time is 0.20 sec, the controller will identify the system instability at time 1.62 sec as Gen 2 will move above the energy bound, and tripping Gen 2 will stabilize the system. The improvement of clearing time is 0.6 cycles.

Table 4-8 Simulation results for the two area system with different load

Clearing time	0.19 sec	0.20 sec	0.21 sec	0.22 sec
Stability	Stable	Unstable	Unstable	Unstable
T_control		1.62 sec	1.41 sec	1.25 sec

(2) Results for the 39 bus system

(a) Here, the results of the 39 bus system with ZIP (30%,30%,40%) load model are listed in table 4-9. Table 4-10 lists the results that the algorithm improves the system stability. Since the system load is decreased, the algorithm is more effective compared to Table 3-4.

Table 4-9 Simulation results for the 39 bus system

Fault Bus	Line Removed	Fault Time(cycles)	Gen tripped	tripping time(sec)
4	4-14	12	10(50%)	1.34
14	4-14	12	10(50%)	1.37
4	4-5	11	10(50%)	1.52
3	3-4	12	10(50%)	1.20
4	3-4	12	10(50%)	1.27
5	5-6	11	2	1.43
6	5-6	10	2	1.56
2	2-25	7	9	1.60
25	2-25	6	9	1.43
16	16-19	5	4,5	0.61
19	19-16	5	4,5	0.57

21	16-21	10	10(50%)	1.26
16	16-21	8	10(50%)	1.03

Table 4-10 Improvement on the system stability

Fault Bus	Line Removed	Fault Time(cycles) improvement
4	4-14	3
14	4-14	3
4	4-5	3
3	3-4	2
4	3-4	2
5	5-6	3
6	5-6	2
2	2-25	2
25	2-25	2
16	16-19	0
19	19-16	0
21	16-21	2
16	16-21	2

(b) Continuing with the previous ZIP (30%, 30%, 40%) load model, we increase the load level to 120% and distribute the load to each generator of the system. Table 4-4 shows the simulation results. The fault time of each fault is the critical time the system becomes unstable. When the first generator moves above its energy threshold, we take a generation tripping in accelerating area; at the same time, we also add load shedding action in decelerating area. In this stressed system, we take the control actions based on the observation of phase angle measurements with the respect of COA. In each unstable case, Gen 10 is the one which decelerates from COA, so we shed 50% load (600MW) at the Bus 39 which is the terminal bus of Gen 10 at the time the first generator moves beyond threshold. Table 4-11 and Table 4-12 list the simulation results.

Table 4-11 Simulation results for the 39 bus system in a stress condition

Fault Bus	Line Removed	Fault Time(cycles)	Gen tripped	tripping time(sec)
4	4-14	7	2,3	0.98
14	4-14	7	2,3	0.93
4	4-5	6	2,3	1.01
3	3-4	7	2,3	0.99
4	3-4	7	2,3	1.02
5	5-6	6	2	1.10
6	5-6	5	2	1.15
2	2-25	6	9	1.13
25	2-25	5	9	0.98
16	16-19	5	4,5	0.57
19	19-16	5	4,5	0.53
21	16-21	7	2,3	1.03
16	16-21	6	2,3	0.94

Table 4-12 Improvement on the system stability

Fault Bus	Line Removed	Fault Time(cycles) improvement
4	4-14	0
14	4-14	0
4	4-5	0
3	3-4	1
4	3-4	1
5	5-6	0
6	5-6	0
2	2-25	1
25	2-25	1
16	16-19	0
19	19-16	0
21	16-21	1
16	16-21	1

4.4 COMPARISON AND DISCUSSION

Two new algorithms are proposed with the concept of synchrophasors measurements in this thesis. The first method uses bus voltage phase angle measurements to detect the system instability, and the second method is developed with the concept of

energy function which needs measurements of generator power, mechanical torque, bus frequency, besides bus voltage phase angle. Therefore, the second algorithm will detect the system instability more accurately and generally, especially, with the consideration of frequency.

In the two area system, we remove the governors and set up a three phase fault on Bus 8. Figure 4-7 and Figure 4-8 are the angle and energy of each generator, respectively. Figure 4-9 gives out the speed of the four generators. For this simple example, using only phase angle measurements gives out a stable result, while actually the generators are speeding up. Thus, using energy function can avoid this kind of detecting error.

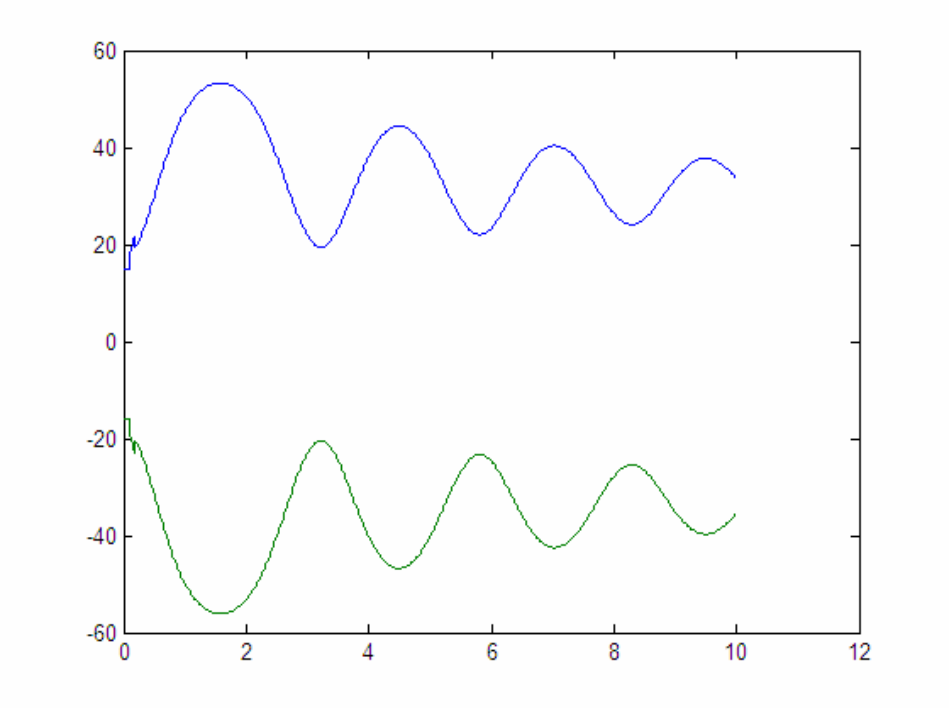

Figure 4-7 Angles of generators without governors

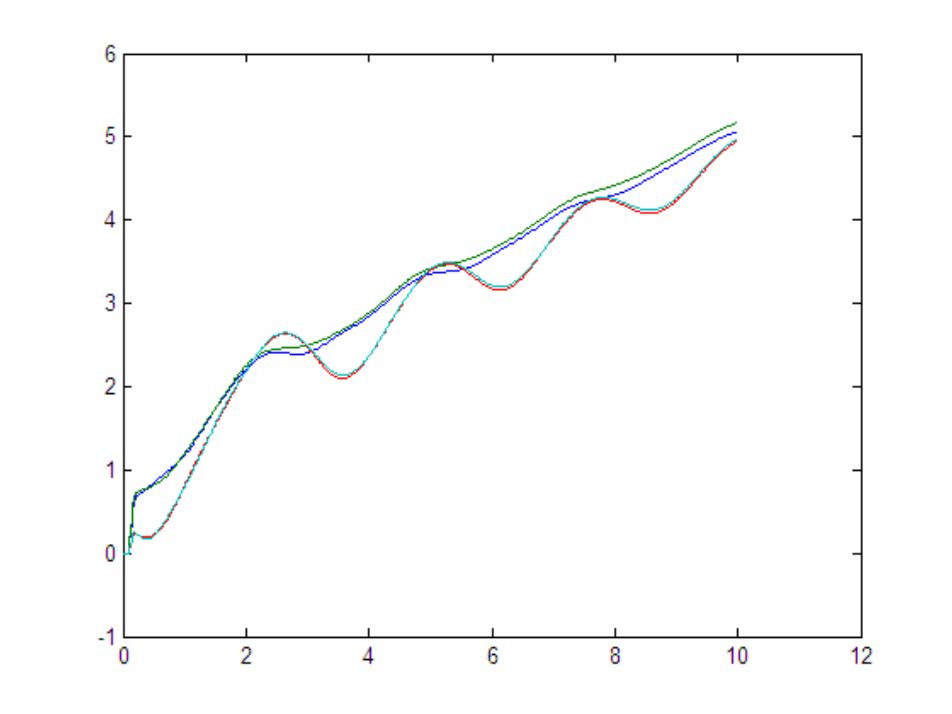

Figure 4-8 Total energy of each generator without governors

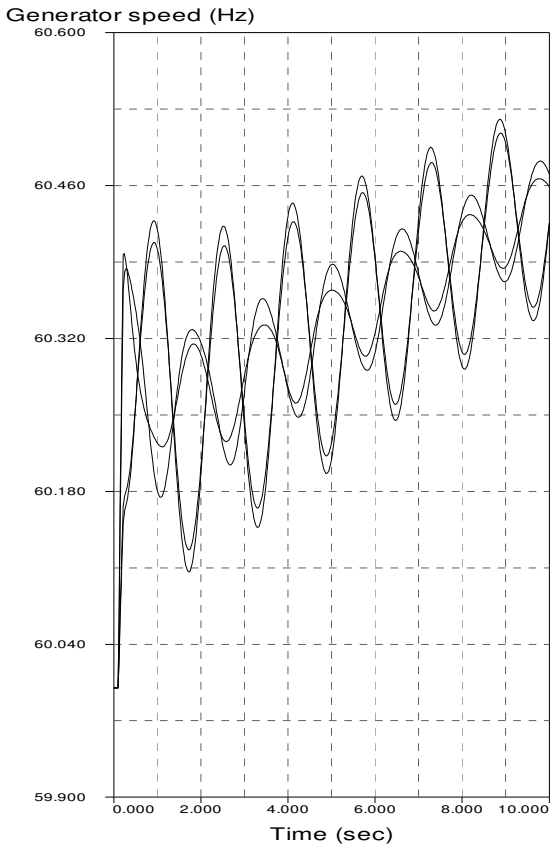

Figure 4-9 Generator speeds without governors

Considering such a case, in the 39 bus system, suppose a generator tripping at time 0.1 second, the system frequency will drop due to the loss of generation. When we trip Gen 2 and Gen 4 at time 0.1 second, Figure 4-10 shows the frequency of the generators. If we use the first algorithm, since the angles will not depart from each other, Figure 4-11 shows the algorithm result. Now, we use the algorithm based on the energy function, the energy of each generator is shown in Figure 4-12, and Gen 10 will move above the energy bound at time 2.8 second. Since the system frequency is below 60 Hz, we need to take the control as load shedding at the Bus near Gen 10. After the load shedding, the frequency of the generators is shown in Figure 4-13. The discussions above show that the energy function algorithm takes advantage with the frequency considered.

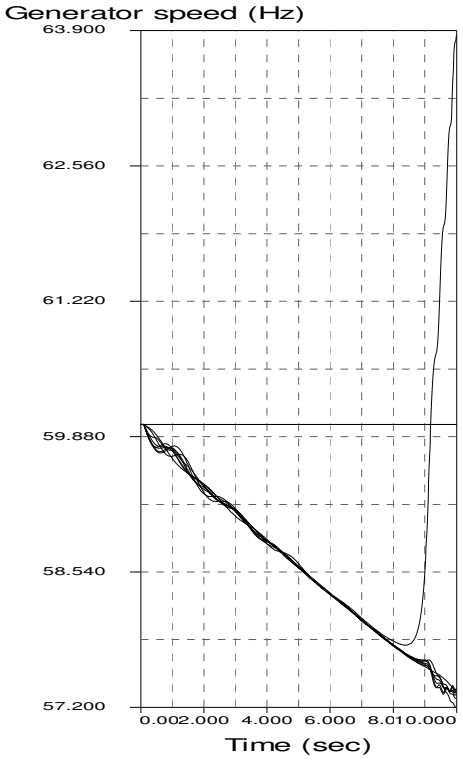

Figure 4-10 Frequency of generators when tripping Gen 2 and Gen 4

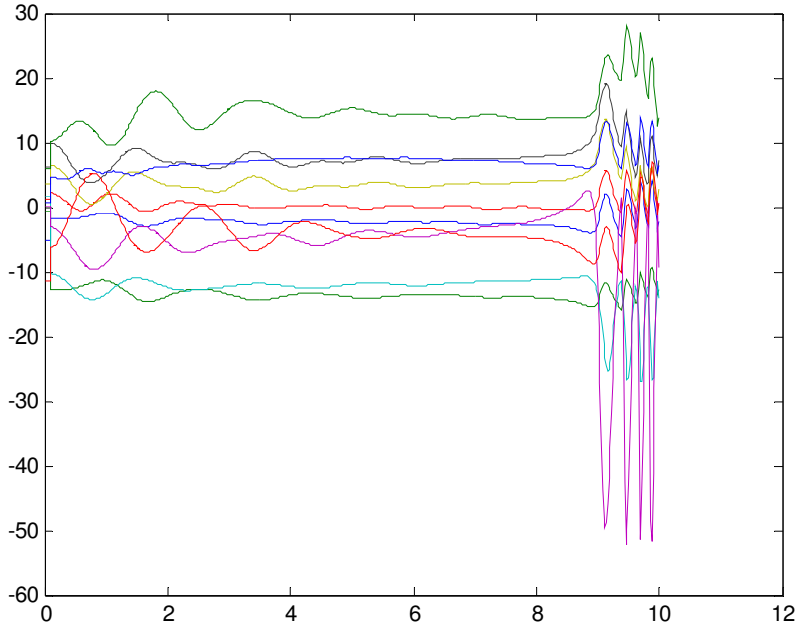

Figure 4-11 Angles of generators when tripping Gen 2 and Gen 4

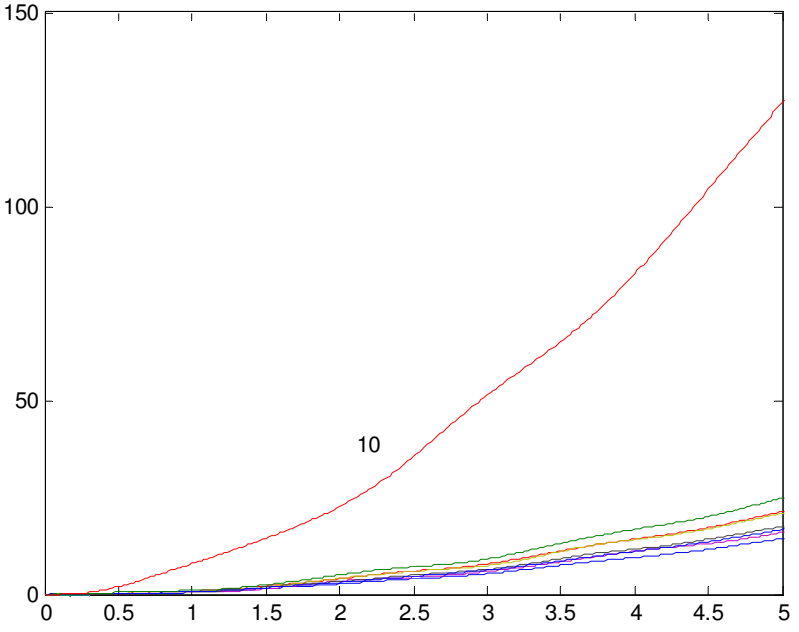

Figure 4-12 Total energy of each generator when tripping Gen 2 and Gen 4

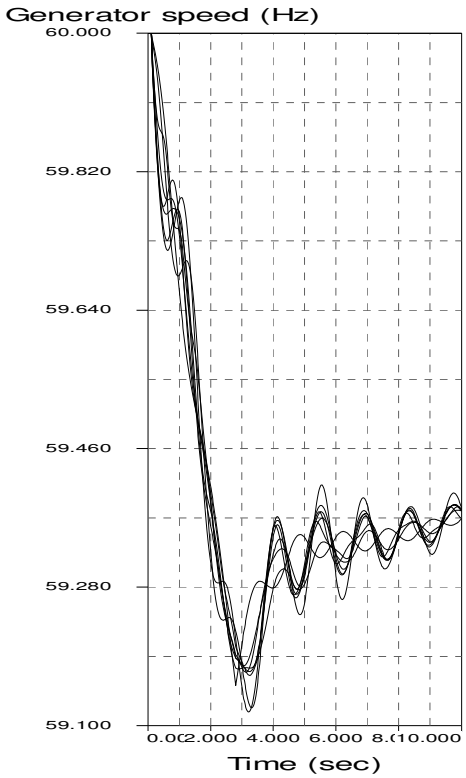

Figure 4-13 Frequency of generators after load shedding

Recall Table 2-3 and Table 3-3, comparison is listed in table 4-13. From the table, we could see that the first algorithm is much faster than the second one, which means it could save more control time for the system. The integration of the potential energy slows down the speed of the second algorithm. In the real system, system frequency is well monitored and controlled with AGC and other devices. Using only phase angle measurements is easy to implement and fast for detecting the system instability.

Table 4-13 Comparison of two algorithms

Fault Bus	Line Removed	Fault Time(cycles)	Gen tripped	Tripping time(sec)	
				Algorithm1	Algorithm2
4	4-14	13	10	0.76	1.09
14	4-14	13	10	0.78	1.13
4	4-5	12	10	0.88	1.31
3	3-4	12	10	0.73	0.99
4	3-4	11	10	0.84	1.03
5	5-6	11	2	0.90	1.23

6	5-6	10	2	1.11	1.37
2	2-25	7	9	1.06	1.41
25	2-25	6	9	0.92	1.32
16	16-19	5	4,5	0.52	0.58
19	19-16	5	4,5	0.46	0.52
21	16-21	9	10	0.90	1.02
16	16-21	7	10	0.77	0.92

.

4.5 CONCLUSION

Different simulation conditions are discussed in this chapter. The two algorithms are compared in the test system. The simple, fast and stable algorithm using bus voltage phase angle measurements appears to show advantages over the energy function method.

CHAPTER 5 CONCLUSION

This thesis presents algorithms for processing of phase angle measurements from across the system to decide whether any part or any control area within the system is speeding away from the rest. When the angle separations go above preset thresholds, remedial actions such as generation and load tripping are ordered by the stability controller to keep the areas in synchronism. This algorithm is meant to be a safety net when the normal RAS or SPS schemes have failed to operate for whatever reason and when the system is beginning to separate into islands. The proposed algorithm and the controller detect the fast separation of phase angles among the critical areas automatically using the synchrophasors and proceed to mitigate the instability by suitable switching actions. The thesis tests the new algorithm with illustrative examples on standard IEEE test systems.

This thesis also proposes the algorithm using real-time computation of energy functions to detect the system instability. When the system has large transient behaviors, the energy of the critical generators will move above their energy bound. This algorithm detects the critical generator's energy and leads to some witching controls. The energy function algorithm is also tested on standard IEEE test systems.

Different simulation conditions are discussed in this thesis and the two new algorithms are compared. The simple, fast and stable algorithm using bus voltage phase angle measurements takes advantage.

This thesis proposes the algorithm which could detect the system instability and send out proper control actions. But how much the amounts of the tripping generation or load shedding should be still needs to be further analyzed in future work. The

computation and set-up of the thresholds of both algorithms are also need accurate analysis in real-time system.

REFERENCES

[1] C. Taylor, D. Erickson, B. Wilson, and K. Martin. (2002, December 16). Wide-Area Stability and Voltage Control System (WACS) Demonstration.

[2] U.S.–Canada Power System Outage Task Force, "Causes of the August 14th Blackout in the United States and Canada," Interim Rep., Nov. 2003, Ch 6.

[3] "Final report on the August 14, 2003 blackout in the United States and Canada: Causes and recommendations," US–Canada Power System Outage Task Force, 2004.

[4] C. W. Taylor and D. C. Erickson, "Recording and analyzing the July 2 cascading outage," IEEE Computer Applications in Power, pp. 26-30, vol. 10, January 1997.

[5] P. Kundur, Power System stability and control, McGraw-Hill, 1994

[6] C. W. Taylor, Power system Voltage Stability, McGraw-Hill, 1994

[7] K. Tomsovic, D. Bakken, V. Venkatasubramanian, A. Bose, "Designing the Next Generation of Real-Time Control, Communication and Computations for Large Power Systems," IEEE Proc. – Special Issue on Energy Infrastructure Systems, Proceedings of IEEE, vol. 93, no. 5, May 2005.

[8] C. Rehtanz, J. Bertsch, "Wide Area Measurement and Protection System for Emergency Voltage Stability Control,"Power Engineering Society Winter Meeting, 2002. IEEE, vol. 2, pp. 842 – 847, Jan 2002.

[9] Taylor, C.W., "The Future in On-Line Security Assessment and Wide-Area Stability control," Power Engineering Society Winter Meeting, 2000. IEEE, vol. 1, pp. 78 - 83 Jan 2000.

[10] E. Nobile, A. Bose, and K. Tomsovic, "Feasibility of a bilateral market for load following," IEEE Trans. Power System., vol. 16, no.4, pp. 782–787, Nov 2001.

[11] X. Yu and K. Tomsovic, "Application of linear matrix inequalities for load frequency control with communication delays," IEEE Trans. Power System, vol. 19, no. 3, pp. 1508–1515, Aug 2004.

[12] S. Bhowmik, K. Tomsovic, and A. Bose, "Communication models for third party load frequency control," IEEE Trans. Power System, vol.19, no. 1, pp. 543–548, Feb 2004.

[13] J. P. Paul, J. T. Leost, and J. M. Tesseron, "Survey of the secondary voltage control in France: Present realization and investigations," IEEE Trans. Power System, vol. PWRS-2, no. 2, pp. 505–511, May 1987.

[14] S. Corsi, P. Marannino, N. Losignore, G. Moreschini, and G. Piccini, "Coordination between the reactive power scheduling function and the hierarchical voltage control of the EHV ENEL system," IEEE Trans. Power Syst., vol. 10, no. 2, pp. 686–694, May 1995.

[15] H. Vu, P. Pruvot, C. Launay, and Y. Harmand, "An improved voltage control on large scale power system," IEEE Trans. Power Syst., vol. 11, no. 3, pp. 1295–1303, Aug. 1996.

[16] A. Zobian and M. Ilic, "A steady state voltage monitoring and control algorithm using localized least square minimization of load voltage deviations," IEEE Trans. Power Syst., vol. 11, no. 2, pp.929–938, May 1996.

[17] C. Yu, Y. T. Yoon, M. Ilic, and A. Catelli, "On-line voltage regulation: The case of New England" IEEE Trans. Power Syst., vol. 14, no. 4, pp. 1477–1484, Nov. 1999.

[18] Y. Chen, "Development of automatic slow voltage control for large power systems," Ph.D. dissertation, Washington State Univ., Pullman, 2001.

[19] Yi Zhang; Tomsovic, K, **"**Adaptive remedial action scheme based on transient energy analysis**"**. Power Systems Conference and Exposition, 2004, IEEE PES 10-13, pp. 925 - 931 vol.2, Oct. 2004

[20] CIGRE TF 38-02-17, Advanced Angle Stability Controls, GIGRE Brochure No.155, April 2000.

[21] Kamwa, I.; Grondin, R.; Hebert, Y., "Wide-Area Measurement Based Stabilizing Control of Karge Power Systems-A Decentralized/Hierarchical Approach," Power Systems, IEEE Transactions Volume 16, Issue 1, pp. 136 – 153 Feb 2001

[22] C.W. Taylor, D.C.Erickson, K.E.Martin, R.E.Wilson, and V.Venkatasubramanian, "WACS-Wide-area stability and voltage control system: R&D and online demonstration", Proceedings of the IEEE, Vol.93, No.5, pp. 892-906, May 2005.

[23] P.D. Aylett. "The Energy Integral Criterion of Transient Stability Limits of Power Systems." Proceedings IEEE 105(C), pp. 527-536, 1958,

[24] E.W. Kimbark. "Power System Stability". John Wiley & Sons, Inc., New York, NY. 1945.

[25] T. Athay, V.R. Sherket, R. Podmore, S. Virmani, and C. Puech. "A Practical Method for Direct Analysis of Transient Stability." IEEE Trans. PAS-98, pp. 573-584, 1979,

[26] A. A. Fouad and S. E. Stanton, "Transient Stability of a Multi- machine Power System, Part I: Investigation of System Trajectories," IEEE Transactions PAS-100, pp. 3408-3416, 1981.

[27] A. A. Fouad and S. E. Stanton, “Transient Stability of a Multi- machine Power System, Part 11: Critical Transient Energy,” IEEE Transactions PAS-100, pp. 3417-3424, 1981.

[28] Michel, A. Fouad, A. Vittal, V., “Power system transient stability using individual machine energy functions”, Circuits and Systems, IEEE Transactions on Volume 30, Issue 5, pp. 266 – 276, May 1983.

[29] S. E. Stanton, “Transient Stability Monitoring for Electric Power Systems Using Partial Energy Functions,” IEEE Transactions on Power Systems, Vol. 4, No. 4, pp. 1389-1395, 1989.

[30] S. E. Stanton and W. P. Dykas, “Analysis of a Local Transient Control Action by Partial Energy Functions,” IEEE Transactions on Power Systems, Vol. 4, No. 3, pp. 996-1002, 1989.

[31] A. A. Fouad and V. Vittal. “Power system Transient Stability Analysis Using the Transient Energy Function Method”. Prentice Hall, Inc., 1992.

[32] Stanton, S.E., Slivinsky, C., Martin, K., Nordstrom, J., “Application of phasor easurements and partial energy analysis in stabilizing large disturbances”, Power Systems, IEEE Transactions on Volume 10, Issue 1, pp. 297 – 306, Feb 1995.

[33] Joe H. Chow, Aranya Chakrabortty, Murat Arcak, Bharat Bhargava, and Armando Salazar, “Synchronized Phasor Data Based Energy Function Analysis of Dominant Power Transfer Paths in Large Power Systems”, IEEE Summer Power Meeting, Montreal, Canada, June 2006.

APPENDIX

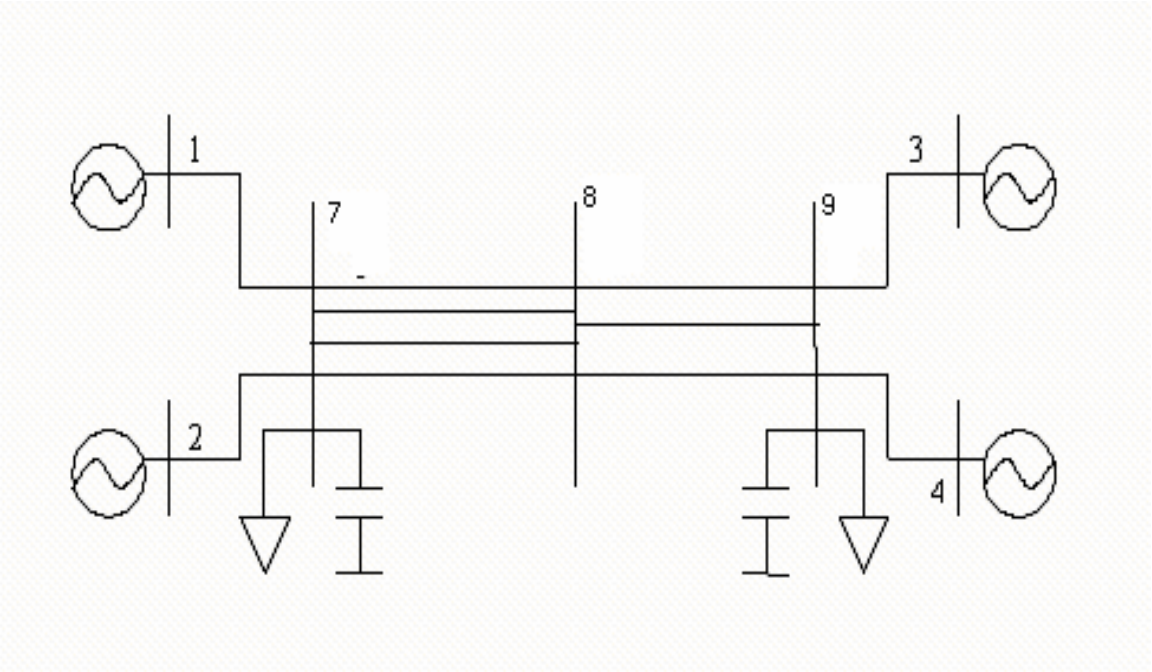

Appendix A Diagram of the two area System

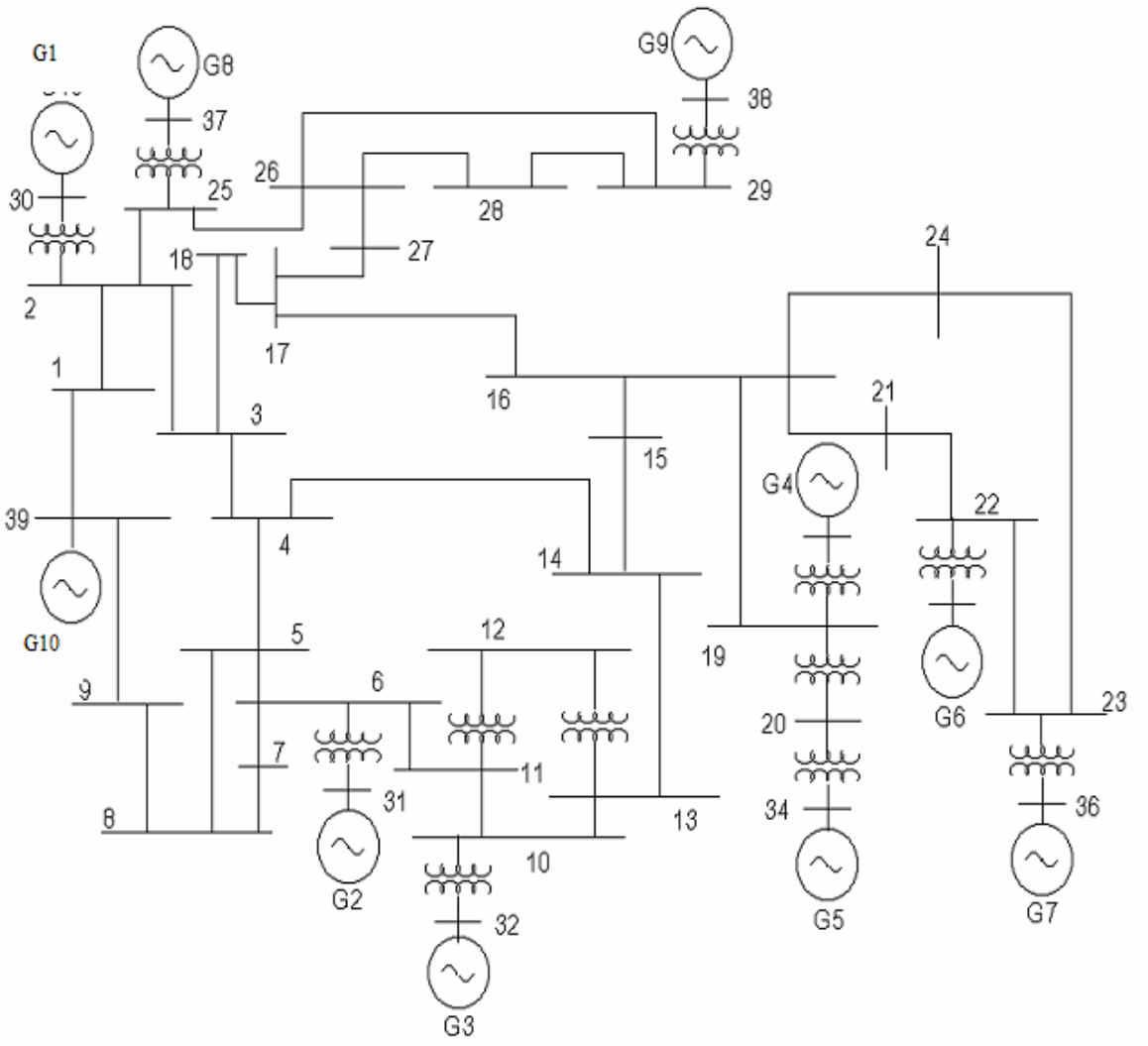

Appendix B Diagram of the 39 bus System